



# UNIVERSITÀ DI PARMA

## ARCHIVIO DELLA RICERCA

University of Parma Research Repository

Laminar Origin of Corticostriatal Projections to the Motor Putamen in the Macaque Brain

This is the peer reviewed version of the following article:

*Original*

Laminar Origin of Corticostriatal Projections to the Motor Putamen in the Macaque Brain / Borra, Elena; Rizzo, Marianna; Gerbella, Marzio; Rozzi, Stefano; Luppino, Giuseppe. - In: THE JOURNAL OF NEUROSCIENCE. - ISSN 1529-2401. - 41(2021), pp. 1455-1469. [10.1523/JNEUROSCI.1475-20.2020]

*Availability:*

This version is available at: 11381/2891270 since: 2022-01-10T11:25:46Z

*Publisher:*

Society for Neuroscience

*Published*

DOI:10.1523/JNEUROSCI.1475-20.2020

*Terms of use:*

openAccess

Anyone can freely access the full text of works made available as "Open Access". Works made available

*Publisher copyright*

(Article begins on next page)

*Research Articles: Systems/Circuits*

## Laminar origin of corticostriatal projections to the motor putamen in the macaque brain

<https://doi.org/10.1523/JNEUROSCI.1475-20.2020>

**Cite as:** J. Neurosci 2020; 10.1523/JNEUROSCI.1475-20.2020

Received: 9 June 2020

Revised: 1 December 2020

Accepted: 4 December 2020

---

*This Early Release article has been peer-reviewed and accepted, but has not been through the composition and copyediting processes. The final version may differ slightly in style or formatting and will contain links to any extended data.*

**Alerts:** Sign up at [www.jneurosci.org/alerts](http://www.jneurosci.org/alerts) to receive customized email alerts when the fully formatted version of this article is published.

1 **Laminar origin of corticostriatal projections to the motor putamen in the macaque brain**

2 Elena Borra, Marianna Rizzo, Marzio Gerbella, Stefano Rozzi, Giuseppe Luppino

3 Università di Parma, Dipartimento di Medicina e Chirurgia, Via Volturno 39E, 43125 Parma, Italy

4 **Corresponding authors:** Elena Borra. E mail: [elena.borra@unipr.it](mailto:elena.borra@unipr.it)

5

6 **Abbreviated title:** Laminar origin of corticostriatal projections

7 **Keywords:** Basal ganglia; Striatum; Motor control; Striatal input channels; Layer VI; Primates

8

9 **Number of figures and tables:** 10 Figures, 3 Tables

10 **Number of pages:** 33

11 **Number of words:** in abstract (240), introduction (597), discussion (1560)

12

13 **Conflict of interest:** The authors declare no competing financial interests.

14 **Acknowledgements:** This research has financially been supported by the Programme “FIL-Quota  
15 Incentivante” of University of Parma and co-sponsored by Fondazione Cariparma and by Ministero  
16 dell’Istruzione, dell’Università e della Ricerca (Grant number: PRIN 2017, n°2017KZNZLN\_002).

17 The 3D reconstruction software was developed by CRS4, Pula, Cagliari, Italy.

18

19 **ABSTRACT**

20 In the macaque brain, projections from distant, interconnected cortical areas converge in specific  
21 zones of the striatum. For example, specific zones of the motor putamen are targets of projections  
22 from frontal motor, inferior parietal and ventrolateral prefrontal hand-related areas and thus are  
23 integral part of the so-called “lateral grasping network”. In the present study, we analyzed the  
24 laminar distribution of corticostriatal neurons projecting to different parts of the motor putamen.  
25 Retrograde neural tracers were injected in different parts of the putamen in 3 *Macaca mulatta* (one  
26 male) and the laminar distribution of the labeled corticostriatal neurons was analyzed quantitatively.  
27 In frontal motor areas and frontal operculum, where most labeled cells were located, almost  
28 everywhere the proportion of corticostriatal labeled neurons in layers III and/or VI was comparable  
29 or even stronger than in layer V. Furthermore, within these regions, the laminar distribution pattern  
30 of corticostriatal labeled neurons largely varied independently from their density and from the  
31 projecting area/sector, but likely according to the target striatal zone. Accordingly, the present data  
32 show that cortical areas may project in different ways to different striatal zones, which can be  
33 targets of specific combinations of signals originating from the various cortical layers of the areas  
34 of a given network. These observations extend current models of corticostriatal interactions,  
35 suggesting more complex modes of information processing in the basal ganglia for different motor  
36 and non-motor functions and opening new questions on the architecture of the corticostriatal  
37 circuitry.

38

39 **SIGNIFICANT STATEMENT**

40 Projections from the ipsilateral cerebral cortex are the major source of input to the striatum.  
41 Previous studies have provided evidence for distinct zones of the putamen specified by converging  
42 projections from specific sets of interconnected cortical areas. The present study shows that the  
43 distribution of corticostriatal neurons in the various layers of the primary motor and premotor areas  
44 varies depending on the target striatal zone. Accordingly, different striatal zones collect specific  
45 combinations of signals from the various cortical layers of their input areas, possibly differing in  
46 terms of coding, timing and direction of information flow (e.g., feed-forward, or feed-back).

47

48 **INTRODUCTION**

49 Projections from the ipsilateral cerebral cortex are the major source of input to the striatum, the  
50 main input station of the basal ganglia (cortico-basal ganglia-thalamo-cortical) loop.

51 According to early models, different striatal territories are a target of specific cortical regions  
52 and in turn are at the origin of largely segregated basal ganglia-thalamo-cortical loops (Alexander et  
53 al., 1986). Subsequent studies confirmed this view, but also showed up a finer modular organization  
54 in which each main loop consists of several largely segregated closed subloops. In this view, each  
55 subloop originates from, and projects to, individual cortical areas or limited sets of functionally  
56 related areas and involves distinct, relatively restricted striatal zones, which have been referred to as  
57 “input channels” (Strick et al. 1995; Middleton and Strick 2000). The various subloops, because of  
58 their differential cortical origin and termination, could be functionally distinct and their definition is  
59 thus essential for understanding the mode of information processing in the basal ganglia for  
60 different motor and non-motor functions.

61 In this context, one important aspect is the definition of the way in which cortical areas or  
62 sectors contribute to the projections to a specific striatal zone in terms of laminar origin of their  
63 projections. Based on studies carried out in different animal species, it is largely agreed that  
64 corticostriatal (CSt) neurons are typically located mostly in layer V and, in some cases, layer III of  
65 most cortical areas (see Gerfen and Bolam, 2010). In the macaque brain, based on retrograde tracer  
66 injections in the caudate, the contribution of layer III in the temporal and prefrontal cortex was  
67 found to be correlated with the density of CSt labeled cells (Arikuni and Kubota, 1986; Saint-cyr et  
68 al., 1990). Recently, this view has been seriously challenged by data of Griggs et al. (2017), based  
69 on retrograde tracer injections in the head or the tail of the macaque caudate showing that: i) in the  
70 temporal cortex, laminar patterns of CSt projections from a given cortical sector markedly differ  
71 according to the striatal target; and ii) layer VI can heavily contribute to the projections to specific  
72 striatal targets.

73           Accordingly, laminar patterns of CSt projections could be more complex than previously  
74 considered and could represent an important variable to evaluate in defining the possible  
75 contribution of cortical areas to the projections to a specific putaminal zone.

76           In the present study, we addressed this issue focusing on the macaque CSt projections to the  
77 so-called “motor putamen”, i.e., that part of the putamen that is a target of massive projections from  
78 the various subdivisions of the primary motor and premotor areas (frontal motor areas). Previous  
79 studies have provided evidence for converging projections from different sets of frontal and  
80 cingulate motor areas in different parts of the motor putamen (Takada et al., 1998; Nambu, 2011).  
81 Recent data (Gerbella et al., 2016) showing that projections from hand-related ventral premotor,  
82 inferior parietal, and ventrolateral prefrontal areas forming the “lateral grasping network” (Borra et  
83 al., 2017) overlap in two distinct putaminal zones, suggested an even more complex pattern of  
84 converging input for parallel processing of different aspects of motor and non-motor functions.

85           Specifically, based on retrograde tracer injections in different parts of the motor putamen, we  
86 have analyzed the laminar distribution of the labeled CSt neurons. Main aims were to: i) quantify  
87 the contribution of the different cortical layers to the projections to a given relatively restricted  
88 putaminal zone; ii) see whether these contributions vary within the various labeled cortical regions;  
89 iii) assess whether possible differences in laminar distribution patterns are related to the labeled  
90 cells density, the cortical area, or the target putaminal zone.

91

92

93 **METHODS**94 **Subjects, surgical procedures, and selection of the injection sites**

95 The experiments were carried out in three *Macaca mulatta* (Cases 61, 71, and 75, one male), in  
96 which retrograde neural tracers were injected in the putamen. Animal handling as well as surgical  
97 and experimental procedures complied with the European law on the humane care and use of  
98 laboratory animals (directives 86/609/EEC, 2003/65/CE, and 2010/63/EU) and Italian laws in force  
99 regarding the care and use of laboratory animals (D.L. 116/92 and 26/2014), and were periodically  
100 approved by the Veterinarian Animal Care and Use Committee of the University of Parma and  
101 authorized by the Italian Ministry of Health.

102 Before the injection of neural tracers, we obtained scans of each brain using magnetic  
103 resonance imaging (MRI; Cases 71 and 75: 7 T General Electric, Boston, MA; Case 61: 0.22 T  
104 Paramed Medical Systems, Genova, Italy) to calculate the stereotaxic coordinates of the putaminal  
105 target regions and the best trajectory of the needle to reach it.

106 Under general anesthesia (Cases 61 and 71: Zoletil®, initial dose 20 mg/kg, i.m.,  
107 supplemental 5–7 mg/kg/hr, i.m., or Ketamine, 5 mg/kg i.m. and Medetomidine, 0.08–0.1 mg/kg  
108 i.m.; Case 75: induction with Ketamine 10 mg/kg, i.m. followed by intubation, isoflurane 1.5–2%)  
109 and aseptic conditions, each animal was placed in a stereotaxic apparatus and an incision was made  
110 in the scalp. The skull was trephined to remove the bone and the dura was opened to expose a small  
111 cortical region. After tracer injections, the dural flap was sutured, the bone was replaced, and the  
112 superficial tissues were sutured in layers. During surgery, hydration was maintained with saline, and  
113 heart rate, blood pressure, respiratory depth, and body temperature were continuously monitored.  
114 Upon recovery from anesthesia, the animals were returned to their home cages and closely  
115 observed. Dexamethasone (0.5 mg/kg, i.m.) and prophylactic broad-spectrum antibiotics (e.g.,  
116 Ceftriaxone 80 mg/kg, i.m.) were administered pre- and postoperatively, as were analgesics (e.g.,  
117 Ketoprofen 5 mg/kg i.m.).

118



119 **Tracer injections and histological procedures**

120 Based on stereotaxic coordinates, the neural tracers Fast Blue (FB, 3% in distilled water, Dr Illing  
121 Plastics GmbH, Breuberg, Germany) and Cholera Toxin B subunit, conjugated with Alexa 488  
122 (CTB green, CTBg; 1% in 0.01 M phosphate-buffered saline at pH 7.4, Molecular Probes, Thermo  
123 Fisher Scientific, Waltham, MA) were slowly pressure-injected through a stainless steel 31 gauge  
124 beveled needle attached through a polyethylene tube to a Hamilton syringe (Hamilton Company,  
125 Reno NV). In Cases 71 and 75, the injection needle was lowered to the putamen within a guiding  
126 tube, to avoid tracer spillover in the white matter. Table 1 summarizes the locations of the  
127 injections, the injected tracers, and the amounts injected.

128       After appropriate survival periods following the injections (28 days for FB and 14 days for  
129 CTBg), each animal was deeply anesthetized with an overdose of sodium thiopental and perfused  
130 through the left cardiac ventricle consecutively with saline (about 2 L in 10 min), 3.5%  
131 formaldehyde (5 L in 30 min), and 5% glycerol (3 L in 20 min), all prepared in 0.1 M phosphate  
132 buffer, pH 7.4. Each brain was then blocked coronally on a stereotaxic apparatus, removed from the  
133 skull, photographed, and placed in 10% buffered glycerol for 3 days and 20% buffered glycerol for  
134 4 days. In Case 75, the right inferotemporal cortex was removed for other experimental purposes.  
135 Finally, each brain was cut frozen into coronal sections of 60- $\mu\text{m}$  (Cases 61 and 75) or 50- $\mu\text{m}$  (Case  
136 71) thickness.

137       In all cases, sections spaced 300  $\mu\text{m}$  apart - that is one section in each repeating series of 5 in  
138 Cases 61 and 75 and one in series of 6 in Case 71- were mounted, air-dried, and quickly  
139 coverslipped for fluorescence microscopy. Another series of each fifth section (sixth in Case 71)  
140 was processed for visualizing CTBg with immunohistochemistry. Specifically, endogenous  
141 peroxidase activity was eliminated by incubation in a solution of 0.6% hydrogen peroxide and 80%  
142 methanol for 15 min at room temperature. The sections were then incubated for 72 h at 4°C in a  
143 primary antibody solution of rabbit anti-Alexa 488 (1:15000, Thermo Fisher Scientific; RRID:  
144 AB\_221544) in 0.5% Triton, 5% normal goat serum in PBS, and for 1 h in biotinylated secondary

145 antibody (1:200, Vector Laboratories, Burlingame, CA) in 0.3% Triton, 5% normal goat serum in  
146 PBS. Finally, CTBg labeling was visualized using the Vectastain ABC kit and then a solution of  
147 3,3'-diaminobenzidine (50 mg/100ml; DAB, Sigma-Aldrich, St. Louis, MO), 0.01% hydrogen  
148 peroxide, 0,02% cobalt chloride and 0,03% nickel ammonium sulfate in 0.1M phosphate buffer. In  
149 Case 75, a subset of sections spaced 1200  $\mu$ m immunostained for CTBg, were then incubated  
150 overnight at room temperature in a primary antibody solution of rabbit anti-NeuN (1:5000, Cell  
151 Signaling Technology, Danvers, MA; RRID: AB\_2630395) in 0.3% Triton, 5% normal goat serum  
152 in PBS, and for 1 h in biotinylated secondary antibody (1:100, Vector Laboratories) in 0.3% Triton,  
153 5% normal goat serum in PBS. Finally, NeuN positive cells were visualized using the Vectastain  
154 ABC kit and DAB as a chromogen. With this protocol, in the same tissue sections CTBg labeling  
155 was stained black and NeuN positive cells were stained brown. In Case 75, an additional subset of  
156 sections spaced 1200  $\mu$ m through the frontal lobe, were incubated in a primary antibody solution of  
157 anti-Alexa 488 and in a biotinylated secondary antibody solution as described above, followed by  
158 incubation for 1 h in a solution of streptavidin Alexa 488 – conjugated (1:500, Invitrogen) in PBS  
159 with 0.5% Triton. The same sections were then incubated overnight at room temperature in a  
160 primary antibody solution of mouse monoclonal SMI-32 (1:5000; Covance, Princeton, NJ; RRID:  
161 AB\_2315331), in PBS with 0.5% Triton and 2% normal goat serum, and for 1 h in a secondary  
162 antibody solution of goat anti-mouse conjugated with Alexa 568 (1:500, Invitrogen, Thermo Fisher  
163 Scientific), in PBS with 0.3% Triton and 2% normal horse serum. In all cases, one series of each  
164 fifth section (sixth section in Case 71) was stained with the Nissl method (0.1% thionin in 0.1 M  
165 acetate buffer, pH 3.7).

166

#### 167 **Data analysis**

168 *Injection sites, distribution of retrogradely labeled neurons, and areal attribution of the labeling*

169 The criteria used for defining the injection site core and halo and identifying FB and CTBg labeling  
170 have been described in earlier studies (Luppino et al. 2003; Rozzi et al., 2006). The injection sites

171 of Cases 71 and 75 were completely restricted to the putamen. In Case 61, the CTBg injection site  
172 had some involvement ( $<500\ \mu\text{m}$ ) of the white matter just above the putamen (Fig. 1). This white  
173 matter involvement, given its minimal extent and location in close contact with the putamen and  
174 considering that CTB is characterized by a limited uptake by axons of passage (Lanciego, 2015),  
175 should not have affected the results from this case, which were fully comparable with those of the  
176 other cases.

177 The distribution of retrograde labeling in the cortex was analyzed in sections every  $300\ \mu\text{m}$   
178 and plotted in sections every  $1200\ \mu\text{m}$  (Cases 61, 71r, and 75) or  $600\ \mu\text{m}$  (Cases 71l) together with  
179 the outer and inner cortical borders, using a computer-based charting system. Data from individual  
180 sections were also imported into the 3-dimensional (3D) reconstruction software (Demelio et al.  
181 2001) providing volumetric reconstructions of the monkey brain, including connectional and  
182 architectonic data.

183 The criteria and maps adopted for the areal attribution of the labeling were similar to those  
184 adopted in previous studies (see Borra et al., 2017). Specifically, the attribution of the labeling to  
185 the frontal motor, cingulate, and opercular frontal areas was made according to architectonic criteria  
186 previously described (Matelli et al. 1985; 1991; Belmalih et al. 2009).

#### 187 *Quantitative analysis and laminar distribution of the labeling*

188 In all cases, the number of labeled neurons plotted in the ipsilateral hemisphere was counted and the  
189 cortical input to the injected putaminal zone was then expressed in terms of the percentage of  
190 labeled neurons found in a given cortical subdivision, with respect to the overall cortical labeling  
191 found for each tracer injection.

192 In all cases, the laminar distribution of the labeled cells was analyzed quantitatively in pairs or  
193 triplets of close sections (spaced  $300\text{-}600\ \mu\text{m}$ ), taken at different rostrocaudal levels through the  
194 frontal motor and cingulate cortex and the frontal opercular cortex (Fig. 2). Given that in Cases 75  
195 and 71r the labeling distribution was quite similar, the same levels (two sections/level) were  
196 selected: the first level (A) was taken through F1, the second (B) through the caudal part of F3, the

197 third (C) through the middle part of F3 and the fourth (D) through the rostralmost part of F3. In  
198 Case 61, the labeling involved more rostral cortical territories than in Cases 75 and 71r, thus the  
199 caudalmost level analyzed was level B and it was possible to analyze a further rostral level (E)  
200 through areas F6 and F7. In Case 711, the labeling was dense in relatively restricted cortical sectors,  
201 thus the analysis was focused on these regions, at levels corresponding to B, C, and D, and was  
202 carried out in two (level D) or three (levels B and C) sections spaced 600  $\mu\text{m}$ .

203 Quantitative analysis was also carried out in parietal, insular, and prefrontal sectors selected  
204 based on the distribution of the labeling in each case. For analyzing these regions, given that the  
205 laminar distribution of the labeling was apparently very constant, cortical sectors of 2 mm from two  
206 close sections (spaced 300-600  $\mu\text{m}$ ) were analyzed.

207 The selected sections were photographed at 100x magnification through a digital camera  
208 incorporated into the microscope with an automatic acquisition system (NIS-Element; Nikon Co.,  
209 Tokyo, Japan) and labeled neurons were plotted on the microphotographs. In the frontal sections of  
210 Cases 61, 71r, and 75, the entire extent of the frontal motor and cingulate cortex and the opercular  
211 frontal cortex was subdivided in 500  $\mu\text{m}$ -wide cortical traverses perpendicular to the cortical  
212 surface and running through the entire cortical thickness, from the pial surface to the grey-white  
213 matter border. The width of the traverses was defined along a line running at the level of the layers  
214 III-V border. In the frontal sections of Case 711 and in the sections through the parietal, insular, and  
215 prefrontal cortex in all cases, where the labeling was in general less rich, cortical traverses 1 mm-  
216 wide were defined in limited cortical sectors. Furthermore, microphotographs of immediately  
217 adjacent Nissl-stained sections were overlaid and borders between different cortical layers were  
218 then transferred on the plots. Two types of analyses were carried out on the distribution of the  
219 labeled neurons. The first analysis aimed to obtain an estimate of the variations in overall richness  
220 of the labeling within and across the various labeled cortical sectors. To this purpose, we have first  
221 considered the total number of labeled cells observed in each traverse, in the entire cortical  
222 thickness. Then, to compensate for differences in the number of labeled cells due to variations of

223 the cortical thickness between different areas or to oblique cutting of the cortical mantle, the total  
224 number of labeled cells was divided by the cortical thickness, measured from the pial surface to the  
225 grey-white matter border, expressed in millimeters. Thus, the richness of the labeling (“density”)  
226 was expressed for each traverse in terms of number of labeled cells/mm cortical thickness. The  
227 second analysis aimed to quantify the proportion of CSt labeled cells observed in the various layers.  
228 To this aim, for each traverse the labeling was expressed in terms of percentage of labeled neurons  
229 localized in layers II-III, V, and VI.

230       The distribution of labeled neurons was also analyzed qualitatively across consecutive  
231 sections to exclude the possibility that the observed laminar distribution patterns of the labeling  
232 were only apparent, because of an oblique cutting of the cortical mantle.

233

234 **RESULTS**235 **Location of the injection sites and general distribution of labeled CST neurons in the**  
236 **ipsilateral hemisphere**

237 All injections used for this study involved the putaminal region overlying the crossing of the  
238 anterior commissure (AC) at different dorso-ventral levels (Table 1 and Fig. 1). In Cases 75 and 71r  
239 the injection sites were located in a dorsal and a mid-dorsal part of the putamen, respectively, at  
240 about the antero-posterior (AP) level of the AC (Case 75), or slightly rostral (case 71r). According  
241 to the putaminal motor somatotopy (e.g., Alexander and De Long, 1985; Nambu 2011) the injection  
242 site in Case 75 could correspond mostly to the trunk-leg motor representation and in Case 71r to the  
243 arm and trunk-leg motor representation. In Cases 71l and 61, the injection sites were located more  
244 ventrally in the putamen, 2 mm caudal and 1 mm rostral to the center of the AC, respectively. In  
245 Case 71l, the injection site could overlap with the hand and mouth motor representation. In Case 61,  
246 it extended for about 4 mm in dorso-ventral direction and the ventral part could at least partially  
247 overlap with the rostral “hand-related input channel” (Gerbella et al., 2016).

248 As expected, in all cases the majority of labeled cells was located in frontal motor areas (57-  
249 75% of the labeled cells; Table 2) with additional, in several cases relatively robust, projections  
250 from other cortical regions and their distribution in the ipsilateral hemisphere largely varied  
251 depending on the location of the injection site (Figs. 2 and 3).

252 In Cases 75 and 71r the regional distribution of the labeling was quite similar: in both cases  
253 about 62% of the labeled cells were located within frontal motor areas, about 19-22% in the  
254 cingulate cortex and about 12-17% in the parietal cortex. In both cases the strongest input originated  
255 from F1 (primary motor cortex), mostly from the dorsal and medial part, and a very rich labeling  
256 involved the entire extent of F3 (supplementary motor area) and area 24c/d (cingulate motor areas)  
257 mostly in the caudal part, corresponding to area 24d (Table 3). Relatively strong projections  
258 originated also from F2 and, in Case 71r, in which the injection site extended more ventrally, also

259 from F5. In the parietal cortex, in both cases most of the labeling was in the dorsal part of areas SI  
260 and PE and, in Case 71r, also in area PFG.

261 In Case 71l, the labeling was much weaker in the cingulate cortex and mostly confined to the  
262 frontal motor (76%) and parietal (19%) cortex (Table 2). In the frontal cortex, the labeling was very  
263 strong in the ventral premotor cortex, mostly in F5, also extending in the frontal operculum, and in  
264 the mid-ventral part of F1 (Table 3), as expected from the location of the injection site. Relatively  
265 robust labeling was observed in the rostral part of F3, likely involving the arm and face  
266 representation (Luppino et al., 1991). In the parietal cortex, labeled cells were mostly distributed in  
267 the ventral part of SI, and in SII, PF, PFG, and AIP.

268 In Case 61, the cortical labeling was more extensive than in the other three cases, likely  
269 because of its more rostral location and relatively large dorsoventral extent. Specifically, the  
270 labeling very densely involved the ventral premotor, the ventrolateral prefrontal cortex and the IPL  
271 areas PFG, PG and AIP, which likely reflects involvement of the rostral “hand-related input  
272 channel”. The labeling densely involved also F3 (mostly the mid-rostral part), F2, and 24c/d and,  
273 less densely, areas F6, 24a/b and the insula (Tables 2 and 3).

274

### 275 **Laminar distribution of CSt labeled cells in the frontal motor, cingulate and frontal opercular** 276 **cortex**

277 As shown in detail below, in general the laminar distribution pattern of the labeled CSt cells in the  
278 frontal motor and opercular cortex markedly differed across the various labeled zones and very  
279 rarely showed the pattern commonly described in the primate brain, characterized by CSt cells  
280 almost completely confined to layer V. For example, in the frontal motor cortex, in only 8% of the  
281 1009 cortical bins (500  $\mu$ m wide) analyzed in 36 sections from all cases, labeled cells in layer V  
282 were >66% and in 58% of the bins they were <50%. Indeed, labeled cells almost everywhere in  
283 these regions tended to distribute over almost the entire cortical depth, involving, at a variable

284 extent, layers III, V, and VI. Noteworthy, there were also labeled CSt neurons in the underlying  
285 white matter, which have been described in a previous study (Borra et al., 2020).

286 Figure 4 shows the results of the quantitative analysis carried out in sections through F1,  
287 which was very richly labeled in Cases 75, 71r, and 71l. In sections sampled from Cases 75 and 71r,  
288 taken caudally in F1 (Level A, in Figs. 2 and 3), in the granular cingulate area 23 the labeling by far  
289 predominantly involved layer V, as in most of the sampled bins labeled cells in this layer were  
290 >80% in Case 75 and >90% in Case 71r (Fig. 5A and B). In Case 75, at the transition of area 23  
291 with F1, the laminar distribution pattern radically changed, as the proportion of labeled cells in  
292 layers III and VI increased considerably (Fig 5C). For example, in section 108 there were about 12-  
293 13 mm (bins 16-41) in which the proportion of layer V labeled cells was about 40% and that of  
294 either layer III or layer VI was about 30%, whereas in section 109 the proportion of layer VI labeled  
295 cells tended to be about 20%. Interestingly, this pattern remained unchanged despite clear changes  
296 in labeling density, even when it abruptly halved in the range of very few bins (e.g., bins 28-31 in  
297 section 108). In case 71r, the laminar distribution pattern in a sector of F1 similar to that sampled in  
298 Case 75, was somewhat different: the proportion of labeled cells in layer V tended to be higher than  
299 that in layers III and VI, though remaining for the whole extent of F1 in both the sampled sections  
300 at about 50%. In case 71l, F1 was sampled in a triplet of close sections in a more lateral part (Level  
301 B in Figs. 2 and 3), mostly in the bank of the central sulcus, where the labeling in this area was  
302 richest. In all the three samples, the proportion of labeled cells in layer VI tended to be quite low,  
303 but that in layer III was as high or, in several bins, even higher than in layer V, being above 50% in  
304 8 mm out of 13 mm sampled (Fig 5E). A similar pattern was also observed in bins located in the  
305 bank of the central sulcus in Case 75.

306 In all cases, layer V labeled cells in F1 were all relatively small and tended to be densely  
307 packed mainly in the upper part of the layer, corresponding to sublayer Va. In Case 75, SMI-32  
308 immunofluorescence, which reveals neurofilament proteins expressed in subpopulations of layers  
309 III and V pyramids (Hof and Morrison, 1995), including the larger ones in layer Vb in the frontal



310 motor cortex (Geyer et al., 2000; Belmalih et al., 2009), showed that CTBg labeled neurons, though  
311 invading layer Vb, were considerably smaller than larger SMI-32-immunopositive pyramids (cfr.  
312 Fig. 5C and D). The analysis of these double-labeled sections also clearly showed that a high  
313 proportion of CTBg labeled cells was located well below the large layer Vb pyramids, in layer VI.

314       Rostral to F1, the cingulate area 24c/d and the medial premotor cortex corresponding to F3  
315 were sampled at different AP levels together with the adjacent sectors of F1 or F2 (Levels B, C, and  
316 D; Figs. 6-8). Figure 7 shows the results of the analysis carried out in pairs of sections taken in all  
317 cases at about the middle of F3, possibly corresponding to the arm representation of this area (Level  
318 C). In area 24c/d, labeled cells were mainly located in layer V, although, especially in Case 61, in  
319 several bins the proportion of cells located in layers III and VI was about 40%. In Cases 75 and 71r,  
320 the laminar distribution pattern of labeled cells in F3 (Fig. 5F) was substantially similar to that  
321 observed in F1. In Case 61, the percentage of layer V labeled cells was in most of the bins around  
322 40%, in layer III tended to match that of layer V, whereas in layer VI it was lower and quite  
323 variable. In Case 71l, relatively dense labeling was observed in a restricted zone in the mid-rostral  
324 part of F3. Here, in two out of three sampled sections, labeled cells tended to be located mainly in  
325 layer V (about 60%), whereas in one section the proportion of labeled cells in layer VI matched that  
326 in layer V. In F2, the density of labeled cells tended to be lower than in F3 and their laminar  
327 distribution tended to be similar to that observed in F3, though more variable across bins. Similar  
328 laminar distribution patterns were observed in Cases 75, 71r and 61 in the caudal part of areas 24c/d  
329 and F3 (Level B; Fig. 6).

330       At Level D (Figs. 2 and 3), through the rostralmost part of F3, at the border with F6, a  
331 different laminar distribution pattern was observed in Cases 75 and 71r, characterized by a clear  
332 increase in the percentage of labeled cells in layer V, compared to the more caudal levels (Fig. 8).  
333 In Case 61, about 40-50% of the labeled cells was located in layer V and the remaining were almost  
334 equally subdivided in layers III and VI.

335 An additional more rostral level (Level E) was sampled in Case 61 through areas 24c/d and  
336 F6, where rich labeling was located (Fig. 9). The laminar distribution of the labeling was similar to  
337 that observed more caudally in area 24c/d and rostral F3.

338 Accordingly, as observed for F1, there were differences in the laminar origin of CSt  
339 projections from medial and dorsal premotor areas, which were not correlated with the density of  
340 the labeling, but likely with the target putaminal zone.

341 In three cases (61, 71r and 71l) there was rich labeling also in the ventral premotor cortex  
342 (Fig. 10). In Case 61, the laminar distribution of the labeled cells in this region was examined  
343 through F5 and the frontal operculum (levels D and E) and more caudally through F4 (Level C). In  
344 Cases 71l and 71r, the labeling was rich in restricted zones of F5 and F4, which were sampled at  
345 levels D and C, respectively. In Case 61, in the F5 sector buried within the postarcuate bank  
346 (subdivision F5a) labeled cells were by far predominantly located in layer V. This pattern markedly  
347 changed in the F5 sector extending on the convexity cortex (subdivision F5c), where the percentage  
348 of labeled cells located in layer VI considerably increased, matching in several bins that of layer V  
349 (around 40%; Fig. 5G). More ventrally, in the frontal operculum, at Level E, the contribution of  
350 layer VI further increased, reaching in most of the bins percent values of at least 60%, whereas  
351 more caudally (Level D) tended to be similar to that observed for F5c. In F5c and in the frontal  
352 operculum, as well as in all the other frontal motor areas, labeled cells in layer VI, tended to be  
353 more concentrated in the upper part of the layer and included pyramidal and non-pyramidal neurons  
354 (Fig. 5H). Finally, in F4 (Level C) about 50% of the labeled cells was in layer V.

355 In Cases 71l and 71r, the laminar distribution pattern observed in F5a (both cases) and in F4  
356 (Case 71r) was very similar to that described for Case 61. In contrast, the laminar distribution  
357 pattern observed in F5c in Case 71l was markedly different from that observed in Case 61: the  
358 percentage of labeled cells in layer V was by far predominant and that of layer VI was about 10%.  
359 This observation was a further clear example that a given premotor area can project to different  
360 parts of the motor putamen with a differential contribution of the various cortical layers.

361

362 **Laminar distribution of CSt labeled cells in the parietal, insular, and prefrontal cortex**

363 Differently from what was observed in the frontal motor and cingulate cortex and in the frontal  
364 opercular cortex, in the parietal and insular cortex the laminar distribution of the CSt labeled cells  
365 was substantially uniform and characterized by pyramidal cells predominantly confined to layer V,  
366 with some of them in the position of layer IV. Specifically, in the parietal cortex, independently  
367 from the labeled area and from the richness of the labeling, labeled cells in layer V (plus layer IV)  
368 tended to be almost everywhere >80%, with the remaining mostly localized in layer VI (Fig. 5J). In  
369 the insular cortex, labeled cells were by far predominantly located in layer V in Cases 75, 71r, and  
370 71l in which the labeling was relatively poor. In Case 61, in which labeling in the insula was  
371 considerably richer, most of the labeled cells was located in layer V and a variable, but robust  
372 proportion was located in layer VI. This same case was the only one in which relatively rich  
373 labeling was observed in the ventrolateral prefrontal cortex, more densely involving areas 46v and  
374 12r. In this region, the majority of the labeled cells was located in layer V, but as observed in the  
375 insular cortex, there was a relatively robust contribution (up to 40% of the labeled cells) of layer VI  
376 (Fig. 5I).

377

378 **DISCUSSION**

379 The present study shows that CSt projections from frontal motor areas and frontal operculum do not  
380 originate almost exclusively from layer V, as commonly assumed in primate models of CSt  
381 interactions, as almost everywhere in these regions the contribution of layers III and VI to these  
382 projections is comparable or even stronger than that of layer V. Furthermore, laminar distribution  
383 patterns of the CSt projections can largely vary within these regions independently from the  
384 richness of the projections and from the projecting area/field, but likely according to the target  
385 striatal zones.

386 Thus, cortical areas appear to project in different ways to different zones of the striatum, so  
387 that different striatal zones are targets of characteristically weighted laminar projections from the  
388 various input areas. These observations extend current models of CSt interactions and provide an  
389 even more complex picture of the possible mode of information processing in the basal ganglia for  
390 motor and non-motor functions.

391

392 **Laminar origin of CSt projections**

393 The laminar origin of CSt projections has been described in several studies, showing differences  
394 across species. In cats, CSt neurons were observed mostly in layer III (Kitai et al 1976; Oka, 1980;  
395 Royce, 1982), whereas in dogs mostly in layer V or III in prefrontal and motor cortex, respectively  
396 (Tanaka, 1987). In rats, CSt neurons have been observed mostly in layer V, and at a variable extent  
397 across studies in layer III (e.g., Veening, 1980; McGeorge and Faull, 1989; Akitunde and Buxton,  
398 1992; Wall, 2013). In macaques, after putaminal injections, CSt neurons in the motor cortex were  
399 described almost exclusively in layer Va (Jones et al, 1977), or primarily in layer Va, but also in  
400 layers III and Vb (Mc Farland and Haber, 2000; Kaneda et al 2002). After caudate injections, the  
401 labeling in prefrontal cortex was observed primarily in layer V, with a minor contribution from  
402 layer III, correlated with labeling density (Arikuni and Kubota, 1986; Goldmann Rakic and  
403 Selemon, 1986; Saint-Cyr et al 1990; Yeterian and Pandya 1994; Ferry et al., 2000). It is worth

404 noting that in all these studies the laminar distribution of CSt labeled cells has been evaluated only  
405 qualitatively, which could be at the basis of an underestimation of the involvement of layers III and  
406 VI. Furthermore, the lack of quantitative analysis in virtually all studies of CSt projections prevents  
407 comparisons of the contribution of the various layers across different areas, tracer injections and  
408 studies.

409       The commonly assumed notion that CSt neurons in the macaque brain are primarily located in  
410 layer V (Gerfen and Bolam, 2010; Shepherd, 2013) has been challenged by Griggs et al. (2017).  
411 This study showed that projections from specific temporal areas to the caudate head originated  
412 mostly from layer V and occasionally from layer III, whereas projections from the same areas to the  
413 caudate tail originated from layers III and VI. Accordingly, this study first showed that laminar  
414 distribution patterns of CSt projections from a given cortical area can markedly differ according to  
415 the target striatal zone and that, in macaques, layer VI can be a relevant source of CSt projections.

416       Present data, based on quantitative analysis of the laminar distribution of CSt neurons,  
417 confirm and extend these observations showing that also in the frontal motor and in the frontal  
418 opercular cortex CSt neurons are not located primarily in layer V and that layer VI can be a major  
419 source of CSt projections (e.g., area F5c in Case 61). Labeled CSt neurons in layer VI in ventral  
420 premotor cortex were noticed also by McFarland and Haber (2000). Finally, the present data show  
421 that also after tracer injections in different parts of the putamen, different laminar distribution  
422 patterns can be observed in a given cortical area. For example, after the injections in Case 61 and in  
423 Case 711, the laminar distribution patterns of the labeled neurons in area F5 were markedly  
424 different. Laminar distribution patterns can differ also across different fields of the same area, as  
425 observed in F1 and F3. Noteworthy, these patterns did not change depending on the richness of the  
426 labeling. Thus, similarly to the temporal cortex, in the motor cortex laminar distribution patterns of  
427 CSt projections appear to vary according to the target striatal zone.

428       Present data, as well as those of Griggs et al (2017) raise the question of whether this new  
429 model of laminar architecture of CSt projections applies also to other cortical regions. In parietal

430 and cingulate cortex, CSt labeled cells involved almost exclusively or predominantly layer V.  
431 Although the putamen is a major target of CSt parietal projections (Yeterian and Pandya, 1993;  
432 Cavada and Goldman-Rakic, 1991), we cannot rule out the possibility that projections to the  
433 caudate originate also from other layers. In the insular cortex, we observed labeled CSt neurons in  
434 layers V, or V-VI, and Chikama et al. (1997), after injections in the ventral striatum, observed  
435 labeling in the agranular insula involving layer III. In the prefrontal cortex, Griggs et al (2017)  
436 observed differences in CSt projections from layer III to the caudate tail and head and in the present  
437 study we observed CSt neurons mainly in layers V and VI. Accordingly, it seems possible that also  
438 in the prefrontal and insular cortex laminar distribution patterns of CSt projections vary according  
439 to the target striatal zone.

440

#### 441 **Functional considerations**

442 Previous data suggested that specific striatal zones are targets of converging input from  
443 interconnected cortical areas, thus are integral part of specific large-scale functionally specialized  
444 networks (Gerbella et al. 2016; Choi et al., 2017a, 2017b). Present data show that cortical areas may  
445 project in different ways to different striatal zones, suggesting that they are targets of specific  
446 combinations of signals originating from the various cortical layers of the areas of a given network.

447 These observations extend current models of CSt interactions, suggesting much more  
448 complex modes of information processing in the basal ganglia for different motor and non-motor  
449 functions, and opening new questions on the architecture of the CSt circuitry.

450 Rodent studies provided evidence for different populations of neurons located in different  
451 cortical layers and differentially involved in the CSt circuitry: intrathelencephalic neurons, located  
452 in layers III and Va, which also project to other cortical areas, and pyramidal-tract neurons located  
453 in layer Vb, which also project to brainstem and spinal cord (Reiner et al., 2010). However, the  
454 presence of pyramidal-tract neurons in macaques, suggested by Parent and Parent (2006), is not  
455 supported by electrophysiological data (Bauswein et al., 1989). Furthermore, Jones et al. (1977)

456 showed that CSt neurons are smaller than corticospinal neurons and in the present study we have  
457 not observed large layer Vb labeled pyramids.

458       Rodent studies have also provided evidence for inhibitory Somatostatin or Parvalbumin  
459 positive GABAergic CSt neurons located in layers III, V, and VI (Jinno e Kosaka, 2004; Lee et al.,  
460 2014; Rock et al., 2016), which may differentially modulate striatal output and motor activity  
461 (Meltzer et al., 2017). Though long-range projecting GABAergic cortical neurons have been  
462 described in macaques by Tomioka and Rockland (2007), no evidence has been provided so far for  
463 inhibitory CSt neurons. Double-labelling experiments will be necessary in order to verify whether  
464 also in the macaque there are inhibitory CSt neurons as observed in rodents.

465       Current models of cortical circuitry suggest that the various cortical layers display distinct  
466 responses and dynamics (see, Douglas and Martin 2004). Specifically, in the premotor cortex  
467 activity generated by thalamic or cortical input first involves the middle layers and then superficial  
468 and deep layers (Godlove et al., 2014) and in superficial layers neural activity is predominantly  
469 related to choices, whereas in deeper layers to the motor output (Chandrasekaran et al., 2017).  
470 Finally, in frontal areas deep layers appear to modulate the activity of the superficial layers related  
471 to maintaining contents in working memory (Bastos et al., 2018).

472       Thus, different putaminal zones would collect signals originating from similar sets of hand-  
473 related cortical areas, for example the “lateral grasping network”, but differing in term of coding  
474 and timing even when originating from the same area. Furthermore, layers III, V and VI broadcast  
475 signals in different directions (e.g., feed-forward, or feed-back) to other cortical areas of the  
476 network. Accordingly, each striatal zone would be involved in a very specific way in the flow of  
477 information within the cortico-subcortical network.

478       In this context, noteworthy is the observation that layer VI can be a robust source of CSt  
479 projections. Layer VI hosts pyramidal neurons projecting to the thalamus (CT) or to other cortical  
480 areas (CC; see Thompson, 2010). It is thus an open question whether pyramidal layer VI CSt  
481 neurons observed in the present study represent a new class of layer VI pyramids, or they belong to

482 the CT and/or the CC types. After tracer injections in the thalamus and in the caudate, Yeterian and  
483 Pandya (1994) did not find double-labeled neurons in the prefrontal cortex, where CSt labeled cells  
484 were observed almost exclusively in layer V. Thus, this study does not rule out the possibility that  
485 there are indeed layer VI CSt neurons which also project to the thalamus. Accordingly, it is possible  
486 that striatal zones receive from layer VI neurons signals, which are sent also as feed-back signals  
487 either to cortical areas of the network and/or to thalamic nuclei, possibly to the basal ganglia  
488 recipient ones. Further studies are necessary to characterize connectionally and neurochemically  
489 layer VI CSt neurons and to define the possible role of this projection in the basal ganglia circuitry.  
490



491 **REFERENCES**

492 Akintunde A, Buxton DF (1992) Origins and collateralization of corticospinal, corticopontine,  
493 corticorubral and corticostriatal tracts: a multiple retrograde fluorescent tracing study. *Brain Res.*  
494 586:208–218.

495 Alexander GE, DeLong MR (1985) Microstimulation of the primate neostriatum. II.  
496 Somatotopic organization of striatal microexcitable zones and their relation to neuronal response  
497 properties. *J Neurophysiol.* 53:1417–1430.

498 Alexander GE, DeLong MR, Strick PL (1986) Parallel organization of functionally segregated  
499 circuits linking basal ganglia and cortex. *Annu Rev Neurosci.* 9:357–381.

500 Arikuni T, Kubota K. (1986) The organization of prefrontocaudate projections and their laminar  
501 origin in the macaque monkey: a retrograde study using HRP-gel. *J Comp Neurol.* 244:492–510.

502 Bastos AM, Loonis R, Kornblith S, Lundqvist M, Miller EK (2018) Laminar recordings in  
503 frontal cortex suggest distinct layers for maintenance and control of working memory. *Proc Natl*  
504 *Acad Sci U S A.* 115:1117–1122.

505 Bauswein E, Fromm C, Preuss A (1989) Corticostriatal cells in comparison with pyramidal tract  
506 neurons: contrasting properties in the behaving monkey. *Brain Res.* 493:198–203.

507 Belmalih A, Borra E, Contini M, Gerbella M, Rozzi S, Luppino G (2009) Multimodal  
508 architectonic subdivision of the rostral part (area F5) of the macaque ventral premotor cortex. *J*  
509 *Comp Neurol* 512:183–217.

510 Borra E, Gerbella M, Rozzi S, Luppino G (2017) The macaque lateral grasping network: A  
511 neural substrate for generating purposeful hand actions. *Neurosci Biobehav Rev.* 75:65–90.

512 Borra E, Luppino G, Gerbella M, Rozzi S, Rockland KS (2020) Projections to the putamen from  
513 neurons located in the white matter and the claustrum in the macaque. *J Comp Neurol* 528, 453–467

- 514 Cavada C, Goldman-Rakic PS (1991) Topographic segregation of corticostriatal projections  
515 from posterior parietal subdivisions in the macaque monkey. *Neuroscience*. 42:683–696.
- 516 Chandrasekaran C, Peixoto D, Newsome WT, Shenoy KV (2017) Laminar differences in  
517 decision-related neural activity in dorsal premotor cortex. *Nat Commun*. 8:614. Published 2017 Sep  
518 20. doi:10.1038/s41467-017-00715-0
- 519 Chikama M, McFarland NR, Amaral DG, Haber SN (1997) Insular Cortical Projections to  
520 Functional Regions of the Striatum Correlate with Cortical Cytoarchitectonic Organization in the  
521 Primate *J Neurosci*. 17: 9686–9705.
- 522 Choi EY, Ding SL, Haber SN (2017a) Combinatorial inputs to the ventral striatum from the  
523 temporal cortex, frontal cortex, and amygdala: implications for segmenting the striatum. *eNeuro*.  
524 4:ENEURO.0392-17.2017.
- 525 Choi EY, Tanimura Y, Vage PR, Yates EH, Haber SN (2017b) Convergence of prefrontal and  
526 parietal anatomical projections in a connectional hub in the striatum. *Neuroimage*. 146:821–832.
- 527 Demelio S, Bettio F, Gobbetti E, Luppino G. (2001) Three-dimensional reconstruction and  
528 visualization of the cerebral cortex in primates. In: *Data visualization 2001* (Ebert D, Favre J,  
529 Peikert R, eds) pp 147–156. New York, NY, USA: Springer Verlag.
- 530 Douglas RJ, Martin KA (2004) Neuronal circuits of the neocortex. *Annu Rev Neurosci*. 27:419–  
531 451.
- 532 Ferry AT, Ongür D, An X, Price JL (2000) Prefrontal cortical projections to the striatum in  
533 macaque monkeys: evidence for an organization related to prefrontal networks. *J Comp Neurol*.  
534 425:447–470.
- 535 Gerbella M, Borra E, Mangiaracina C, Rozzi S, Luppino G (2016) Corticostriate Projections  
536 from Areas of the "Lateral Grasping Network": Evidence for Multiple Hand-Related Input  
537 Channels. *Cereb. Cortex* 221:59–78.

538 Gerfen CR, Bolam P (2010) The neuroanatomical organization of the basal ganglia. In:  
539 Handbook of basal ganglia structure and function (Steiner H, Tseng KY, eds.), pp 3–32. London:  
540 Academic Press.

541 Geyer S, Matelli M, Luppino G, Zilles K (2000) Functional neuroanatomy of the primate  
542 isocortical motor system. *Anat Embryol* 202:443–474.

543 Godlove DC, Maier A, Woodman GF, Schall JD (2014) Microcircuitry of agranular frontal  
544 cortex: testing the generality of the canonical cortical microcircuit. *J Neurosci.* 34:5355–5369.

545 Goldman-Rakic PS, Selemon LD (1986) Topography of Corticostriatal Projections in Nonhuman  
546 Primates and Implications for Functional Parcellation of the Neostriatum. In *Sensory-Motor Areas  
547 and Aspects of Cortical Connectivity* (Jones EG et al, eds), pp447–466. Plenum Press, New York.

548 Griggs WS, Kim HF, Ghazizadeh A, Costello MG, Wall KM, Hikosaka O (2017) Flexible and  
549 Stable Value Coding Areas in Caudate Head and Tail Receive Anatomically Distinct Cortical and  
550 Subcortical Inputs. *Front Neuroanat.* 11:106.

551 Hof PR, Morrison JH (1995) Neurofilament protein defines regional patterns of cortical  
552 organization in the macaque monkey visual system: a quantitative immunohistochemical analysis. *J  
553 Comp Neurol* 352:161–186.

554 Jinno S, Kosaka T (2004) Parvalbumin is expressed in glutamatergic and GABAergic  
555 corticostriatal pathway in mice. *J Comp Neurol.* 477:188–201.

556 Jones EG, Coulter JD, Burton H, Porter R (1977) Cells of origin and terminal distribution of  
557 corticostriatal fibers arising in the sensory-motor cortex of monkeys. *J Comp Neurol.* 173:53–80.

558 Kaneda K, Nambu A, Tokuno H, Takada M (2002) Differential processing patterns of motor  
559 information via striatopallidal and striatonigral projections. *J Neurophysiol.* 88:1420–1432.

560 Kitai ST, Kocsis JD, Wood J (1976) Origin and characteristics of the cortico-caudate afferents:  
561 an anatomical and electrophysiological study. *Brain Res.* 118:137–141.

562 Lanciego JL (2015) Retrograde Tract-Tracing “Plus”: Adding Extra Value to Retrogradely  
563 Traced Neurons. In: *Neural Tracing Methods: Tracing Neurons and Their Connections* (Arenkiel  
564 BL, ed), pp67-84. New York: Humana Press.

565 Lee AT, Vogt c D, Rubenstein JL, Sohal VS (2014) A class of GABAergic neurons in the  
566 prefrontal cortex sends long-range projections to the nucleus accumbens and elicits acute avoidance  
567 behavior. *J Neurosci.* 34:11519–11525.

568 Luppino G, Matelli M, Camarda RM, Gallese V, Rizzolatti G. (1991) Multiple representations of  
569 body movements in mesial area 6 and the adjacent cingulate cortex: an intracortical  
570 microstimulation study in the macaque monkey. *J Comp Neurol.* 311:463–482.

571 Luppino G, Rozzi S, Calzavara R, Matelli M (2003) Prefrontal and agranular cingulate  
572 projections to the dorsal premotor areas F2 and F7 in the macaque monkey. *Eur J Neurosci* 17:559–  
573 578.

574 Matelli M, Luppino G, Rizzolatti G (1985) Patterns of cytochrome oxidase activity in the frontal  
575 agranular cortex of macaque monkey. *Behav Brain Res* 18:125–136.

576 Matelli M, Luppino G, Rizzolatti G (1991) Architecture of superior and mesial area 6 and the  
577 adjacent cingulate cortex in the macaque monkey. *J Comp Neurol* 311:445–462.

578 McFarland NR, Haber SN (2000) Convergent inputs from thalamic motor nuclei and frontal  
579 cortical areas to the dorsal striatum in the primate. *J Neurosci.* 20:3798–813.

580 McGeorge AJ, Faull RL (1989) The organization of the projection from the cerebral cortex to the  
581 striatum in the rat. *Neuroscience.* 29:503–37.

- 582 Melzer S, Gil M, Koser DE, Michael M, Huang KW, Monyer H. (2017) Distinct corticostriatal  
583 GABAergic neurons modulate striatal output neurons and motor activity. *Cell Rep.* 19:1045–1055.
- 584 Middleton FA, Strick PL (2000) Basal ganglia and cerebellar loops: motor and cognitive circuits.  
585 *Brain Res Brain Res Rev.* 31:236–250.
- 586 Nambu A (2011) Somatotopic organization of the primate basal ganglia. *Front Neuroanat.* 5:26.
- 587 Oka H (1980) Organization of the cortico-caudate projections. A horseradish peroxidase study in  
588 the cat. *Exp Brain Res.* 40:203–208.
- 589 Parent M, Parent A (2006) Single-axon tracing study of corticostriatal projections arising from  
590 primary motor cortex in primates. *J Comp Neurol.* 496:202–213.
- 591 Pettine WW, Steinmetz NA, Moore T (2019) Laminar segregation of sensory coding and  
592 behavioral readout in macaque V4. *Proc Natl Acad Sci U S A.* 116:14749–14754.
- 593 Reiner A, Hart NM, Lei W, Deng Y (2010) Corticostriatal projection neurons - dichotomous  
594 types and dichotomous functions. *Front Neuroanat.* 4:142.
- 595 Reveley C, Gruslys A, Ye FQ, Samaha J, Glen D, Russ B, Saad Z, Seth A, Leopold DA, Saleem  
596 KS (2017) Three-dimensional digital template atlas of the macaque brain. *Cereb Cortex* 27: 4463-  
597 4477.
- 598 Rock C, Zurita H, Wilson C, Apicella AJ (2016) An inhibitory corticostriatal pathway. *Elife.* 9:5.
- 599 Royce GJ (1982) Laminar origin of cortical neurons which project upon the caudate nucleus: a  
600 horseradish peroxidase investigation in the cat. *J Comp Neurol.* 205:8–29.
- 601 Rozzi S, Calzavara R, Belmalih A, Borra E, Gregoriou GG, Matelli M, Luppino G (2006)  
602 Cortical connections of the inferior parietal cortical convexity of the macaque monkey. *Cereb*  
603 *Cortex* 16:1389–1417.

604 Saint-Cyr JA, Ungerleider LG, Desimone R (1990) Organization of visual cortical inputs to the  
605 striatum and subsequent outputs to the pallido-nigral complex in the monkey. *J Comp Neurol.*  
606 298:129–156.

607 Shepherd GM (2013) Corticostriatal connectivity and its role in disease. *Nat Rev Neurosci*  
608 14:278-291

609 Strick PL, Dum RP, Picard N (1995) Macro-organization of the circuits connecting the basal  
610 ganglia with the cortical motor areas. In: *Models of information processing in the basal ganglia*  
611 (Houk G, ed), pp117–130. Boston: MIT Press.

612 Takada M, Tokuno H, Nambu A, Inase M (1998) Corticostriatal projections from the somatic  
613 motor areas of the frontal cortex in the macaque monkey: segregation versus overlap of input zones  
614 from the primary motor cortex, the supplementary motor area, and the premotor cortex. *Exp Brain*  
615 *Res.* 120:114–128.

616 Tanaka D Jr (1987) Differential laminar distribution of corticostriatal neurons in the prefrontal  
617 and pericruciate gyri of the dog. *J Neurosci.* 7:4095–4106.

618 Thomson AM (2010) Neocortical layer 6, a review. *Front Neuroanat.* 4:13.

619 Tomioka R, Rockland KS (2007) Long-distance corticocortical GABAergic neurons in the adult  
620 monkey white and gray matter. *J Comp Neurol.* 505:526–538.

621 Veening JG, Cornelissen FM, Lieven PA (1980) The topical organization of the afferents to the  
622 caudatoputamen of the rat. A horseradish peroxidase study. *Neuroscience.* 5:1253–1268.

623 Wall NR, De La Parra M, Callaway EM, Kreitzer AC (2013) Differential innervation of direct-  
624 and indirect-pathway striatal projection neurons. *Neuron.* 79:347–360.

625 Yeterian EH, Pandya DN (1993) Striatal connections of the parietal association cortices in rhesus  
626 monkeys. *J Comp Neurol.* 332:175–997.

627 Yeterian EH, Pandya DN (1994) Laminar origin of striatal and thalamic projections of the  
628 prefrontal cortex in rhesus monkeys. *Exp Brain Res.* 99:383–398.

629

630 **Table 1.** Animals used, location of injection sites in the putamen, and type and amount of injected  
 631 tracers

Case	Species	Sex	Age	Weight	Hemisphere	AP*	Tracer	Amount
61	<i>M.Mulatta</i>	F	6	4.5	R	+1	CTBg 1%	2 µl
71	<i>M.Mulatta</i>	F	6.5	3.3	L	-2	FB 3%	0.3 µl
					R	+2	CTBg 1%	1 µl
75	<i>M.Mulatta</i>	M	6	3.5	R	0	CTBg 1%	1 µl

632 \*AP level according to the digital atlas of Reveley et al., (2017) in which AP = 0 is at the level of  
 633 the anterior commissure

634  
 635 **Table 2.** Regional distribution (%) and total number (n) of labeled neurons observed following  
 636 tracer injections in the motor putamen

Case	Prefrontal	Cingulate	Frontal motor	Parietal	Insula	Temporal	n. cells
75	0,7	19,4	61,7	16,7	1,6	-	59653
71r	1,6	21,9	61,6	11,9	3	-	60757
71l	0,5	3,4	75,5	18,6	1,2	0,8	36628
61	8,4	18,3	57	7,5	6,1	2,7	105724

637  
 638 **Table 3.** Distribution (%) in the frontal and cingulate motor cortex and in the frontal operculum  
 639 (FrOp) of labeled neurons observed following tracer injections in the motor putamen

Case	24c/d	F6	F7	F3	F2	FrOp	F5	F4	F1
75	14,4	0,8	0,3	12,7	7,1	2,2	2,5	2,0	34,1
71r	14,4	0,8	0,5	13,2	6,5	2,4	7,9	3,3	26,9
71l	2,5	0,1	-	6,9	0,7	7,6	33,4	8,2	18,6
61	12,3	3,7	1,2	10,6	9,3	16,5	10	3,0	2,7



642 **FIGURE LEGENDS**

643 **Figure 1.** Location of the injection sites. **Upper part:** drawings of coronal sections showing the  
644 location of the injection sites in the putamen depicted as a black zone corresponding to the core,  
645 surrounded by a grey zone corresponding to the halo. All sections are shown as from a right  
646 hemisphere. The anteroposterior (AP) level of the sections is indicated in relation to the digital atlas  
647 of Reveley et al. (2017) in which AP = 0 is at the level of the anterior commissure (AC). **Lower**  
648 **part:** fluorescence photomicrographs of the injection sites in the putamen; scale bar in Case 75  
649 applies to all. Dashed lines in the injection site of Case 61 indicate the deposit of the tracer in  
650 adjacent sections. C, central sulcus; Cd, caudate nucleus; Cg, cingulate sulcus; GP, globus pallidus;  
651 ic, internal capsule; L, lateral fissure; OT, optic tract; Pt, putamen; RTh, reticularis thalami; S, spur  
652 of the arcuate sulcus; ST, superior temporal sulcus.

653 **Figure 2.** Distribution of the cortical labeling observed after injections in the putamen. The  
654 distribution of the retrograde labeling is shown in dorsolateral and medial views of the 3D  
655 reconstructions of the injected hemispheres in which each dot corresponds to one labeled neuron. In  
656 each reconstruction, solid lines indicate the levels (A-E) of the sections selected for the quantitative  
657 analysis. For the sake of comparison, also Case 711 is shown as right. FrOp, frontal operculum; IA,  
658 inferior arcuate sulcus; IP, intraparietal sulcus; LO, lateral orbital sulcus; Lu, lunate sulcus; P,  
659 principal sulcus; ParOp, parietal operculum; SA, superior arcuate sulcus. Other abbreviations as in  
660 Figure 1.

661 **Figure 3.** Distribution of the cortical labeling in one representative section from each level selected  
662 for the quantitative analysis. Section drawings are in a caudal to rostral order (A-E) and were taken  
663 at the levels shown in Figure 2. Section number is indicated in brackets. Arrowheads indicate  
664 borders of frontal motor areas. Subcortical labeling is not shown. A, amygdala; FEF, frontal eye  
665 field; I, insula; ITG, inferior temporal gyrus; LG, lateral geniculate nucleus; Ri, retro-insular cortex;  
666 STG, superior temporal gyrus; Th, thalamus. Other abbreviations as in Figures 1 and 2.

667 **Figure 4.** Percent laminar distribution and density of the retrograde labeling in F1. Graphs show  
668 data from Cases 75, 71r (level A, 2 sections each) and 711 (level B, 3 sections). For each case, on  
669 the left, one section drawing shows the analyzed cortical sector and layer V shaded in light blue.  
670 Graphs from Cases 75 and 71r are aligned at the level of the fundus of the cingulate sulcus (a),  
671 indicated by a vertical dashed line. The other vertical dashed lines indicate the level of the medial  
672 edge of the hemisphere (b) and the shoulder of the central sulcus (c). Graphs from Case 75 and 71r  
673 show data from 500  $\mu\text{m}$ -wide bins from the region in which the labeled cell density was constantly  
674 higher than 10 labeled cells/bin/mm. In graphs from Case 711, the bins are 1 mm-wide and located  
675 in the lateral part of F1, in the bank of the central sulcus. Arrowheads indicate the location of areal  
676 borders.

677 **Figure 5.** Examples of laminar distribution of the labeling. A, B (section 110), C, D (section 106)  
678 and F (section 93) are from Case 75. B and D show the SMI-32 immunofluorescence in A and C,  
679 respectively. E (section 98) is from Case 711. G (section 76, enlarged in H) and I are from Case 61.  
680 J is from Case 71r.

681 **Figure 6.** Percent laminar distribution and density of the retrograde labeling in the cingulate and  
682 frontal motor cortex at level B in Cases 75, 71r and 61. Conventions as in Figure 4.

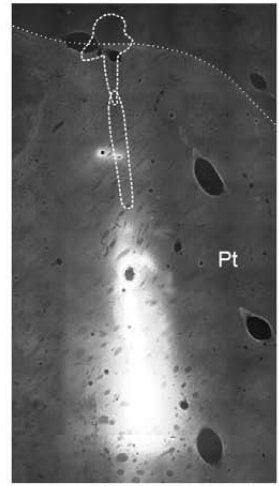
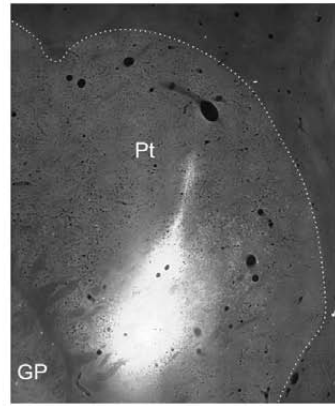
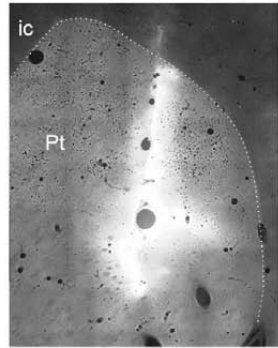
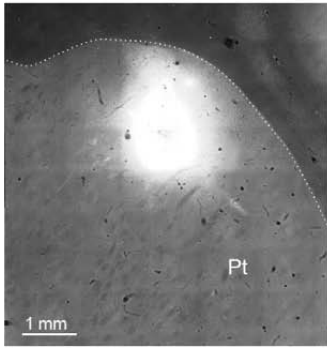
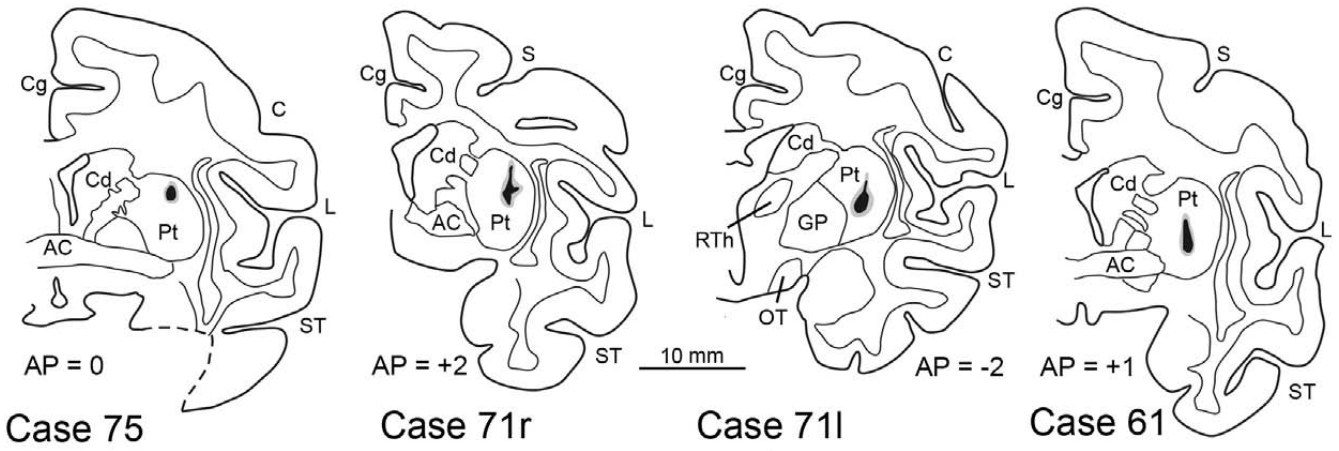
683 **Figure 7.** Percent laminar distribution and density of the retrograde labeling in the cingulate and  
684 frontal motor cortex at level C, in all cases. Conventions as in Figure 4.

685 **Figure 8.** Percent laminar distribution and density of the retrograde labeling in the cingulate and  
686 frontal motor cortex at level D, in Cases 75, 71r and 61. Conventions as in Figure 4.

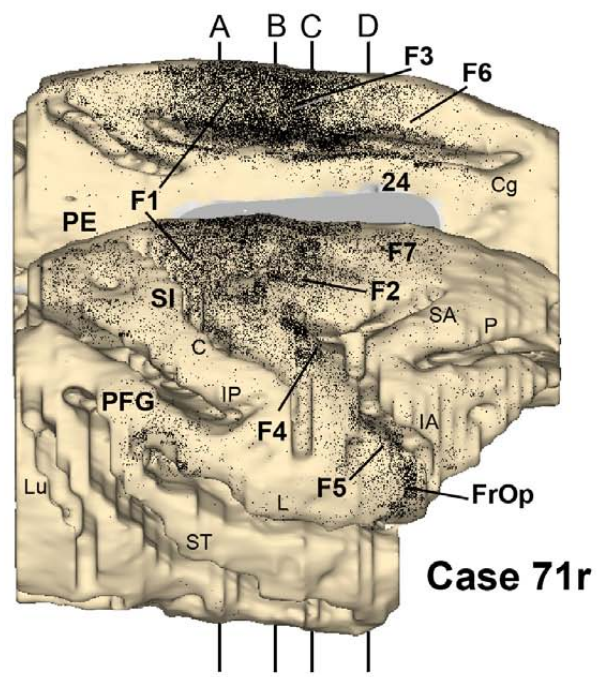
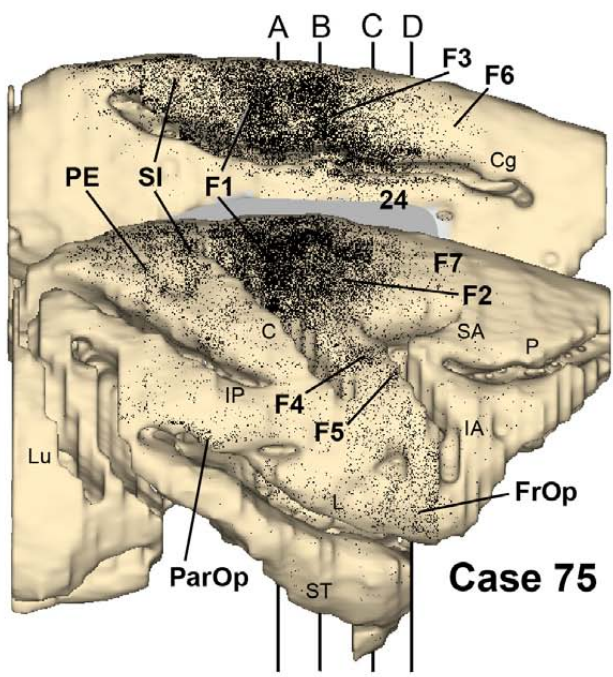
687 **Figure 9.** Percent laminar distribution and density of the retrograde labeling in the cingulate and  
688 frontal motor cortex at level E in Case 61. Conventions as in Figure 4.

689 **Figure 10.** Percent laminar distribution and density of the retrograde labeling in the ventral  
690 premotor and opercular frontal cortex. Graphs from Case 61 show data from a cortical region of

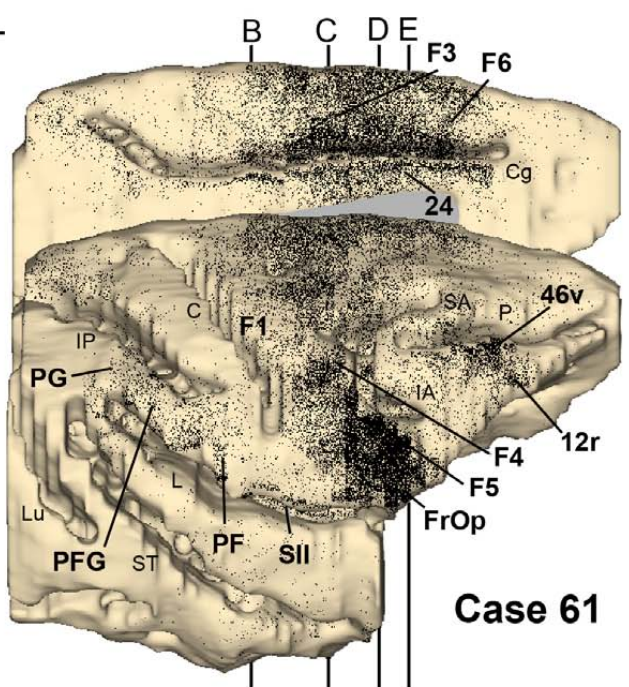
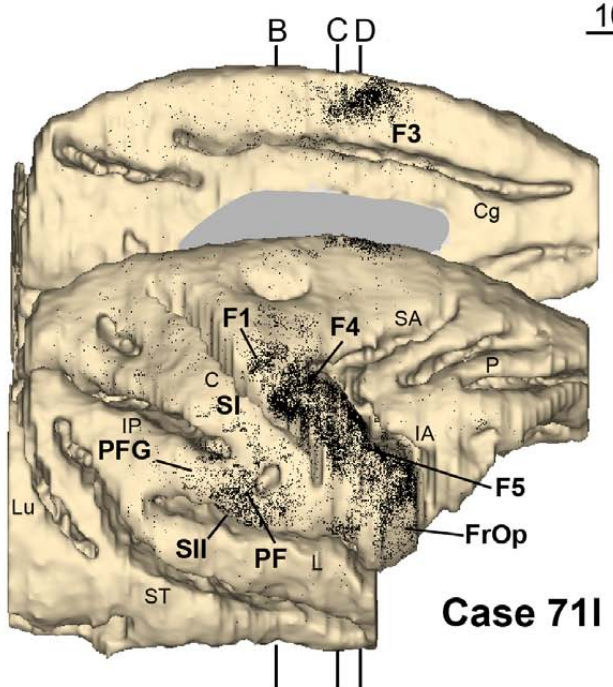
691 sections at levels E and D running from the fundus of the arcuate sulcus (left) through F5a, F5c, and  
692 the frontal operculum and at level C through F4 on the convexity cortex. Graphs from Case 711  
693 show data from cortical sectors 3 mm wide of sections taken at level D within the arcuate bank  
694 (F5a) or on the convexity cortex (F5c). Graphs from Case 71r show data from cortical sectors taken  
695 at level D (in F5a) and level C (in F4) in which the density of labeled cells was above 10  
696 cells/bin/mm. Conventions as in Figure 4.





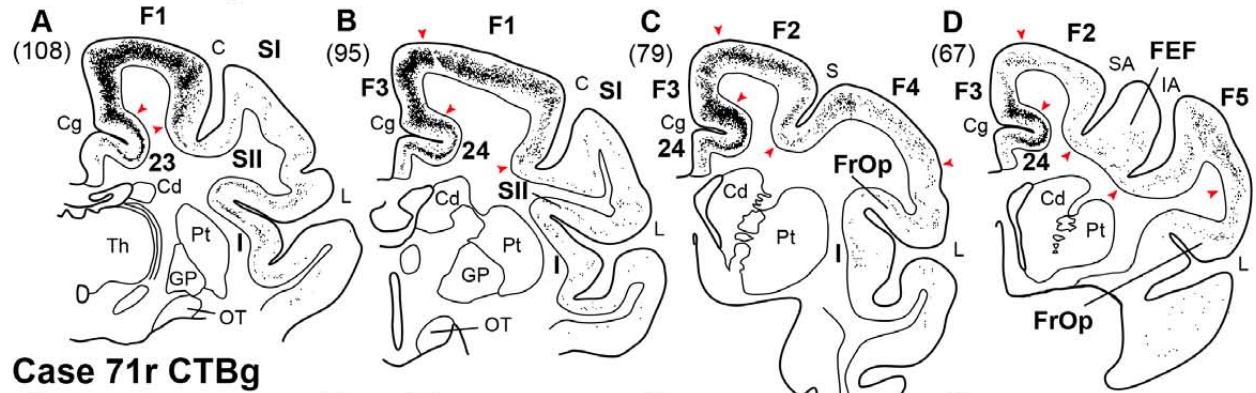


10mm

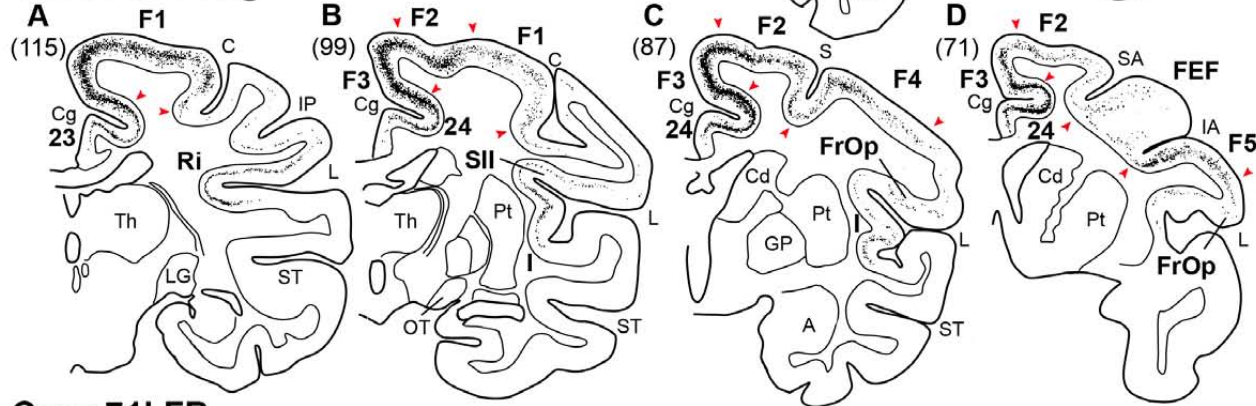




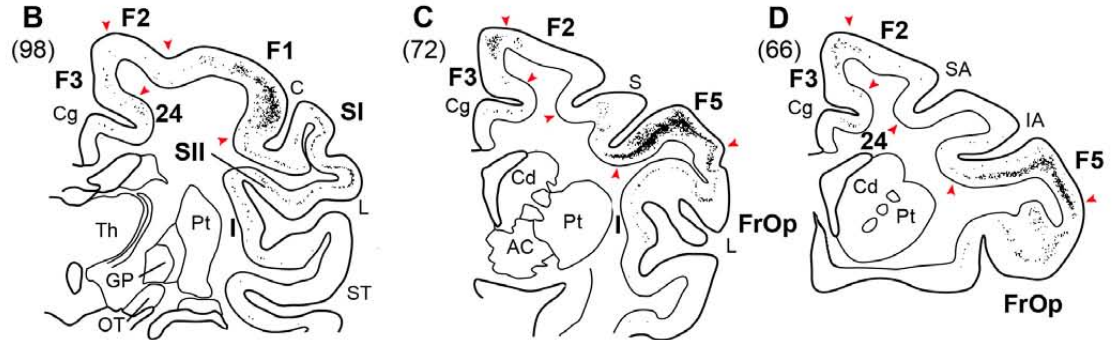
**Case 75 CTBg**



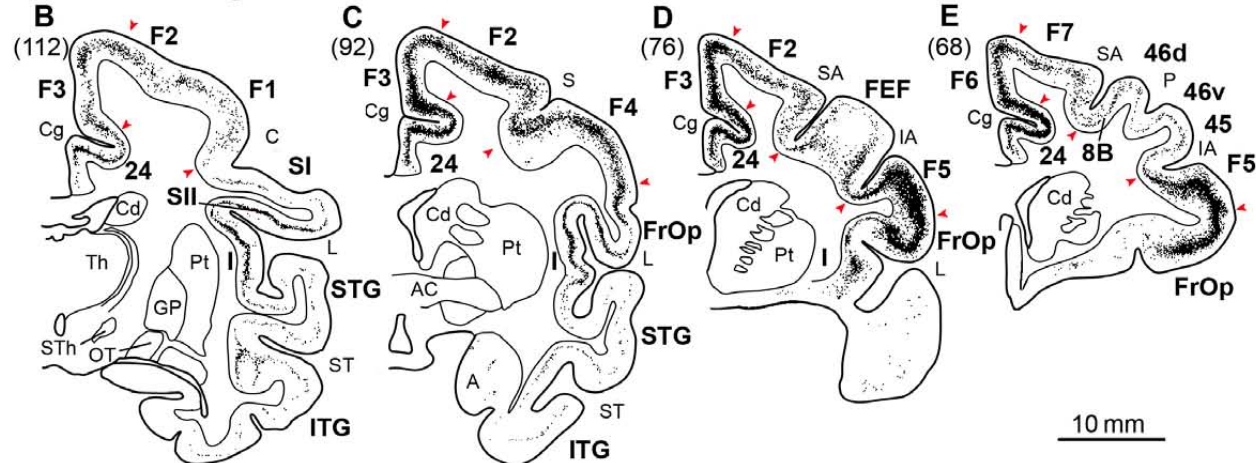
**Case 71r CTBg**

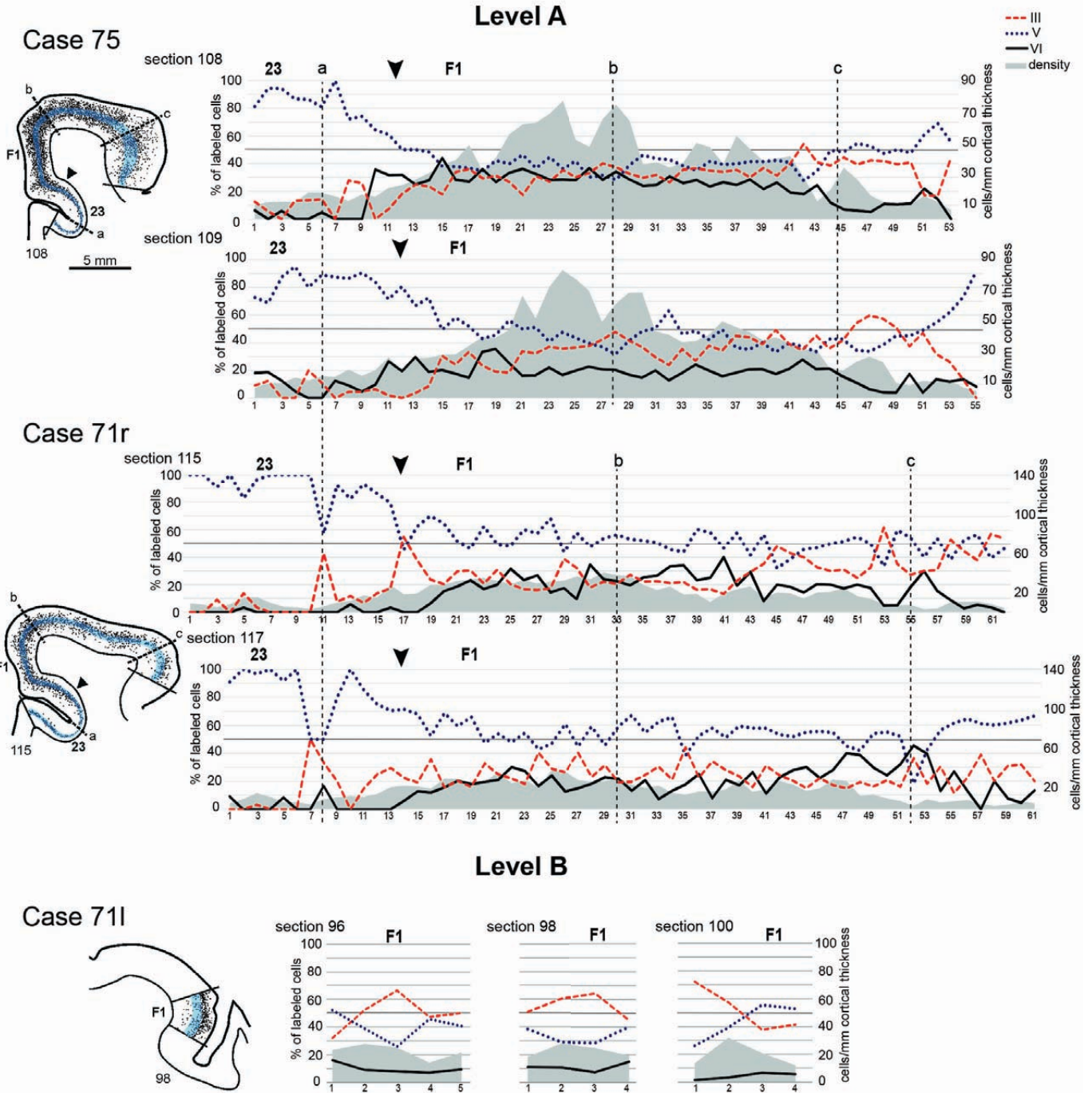


**Case 71l FB**

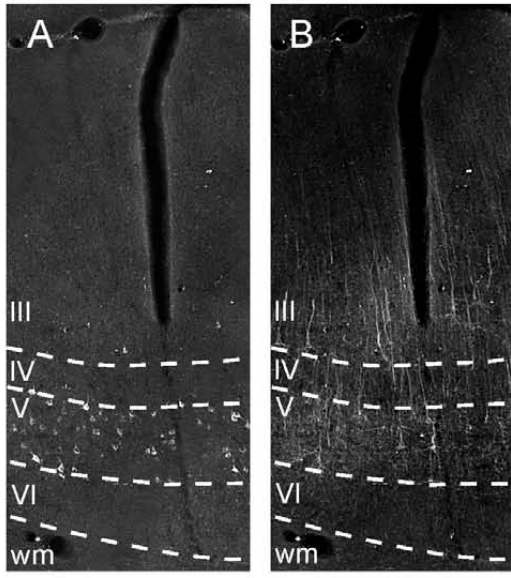


**Case 61 CTBg**

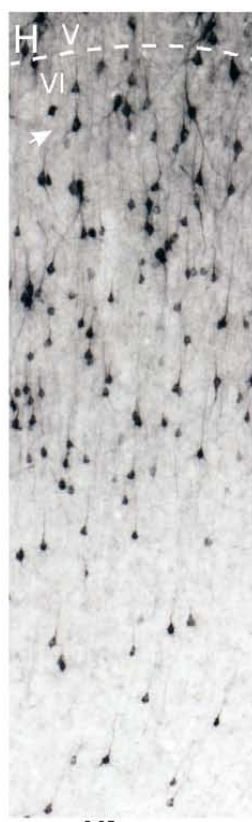
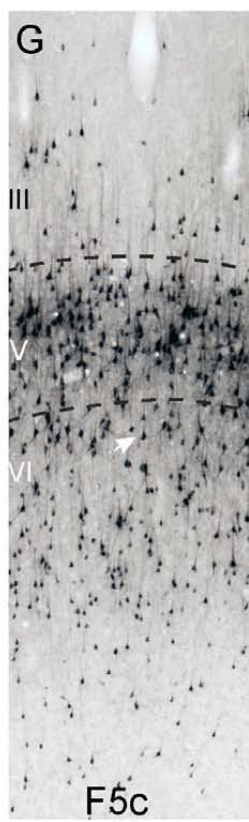
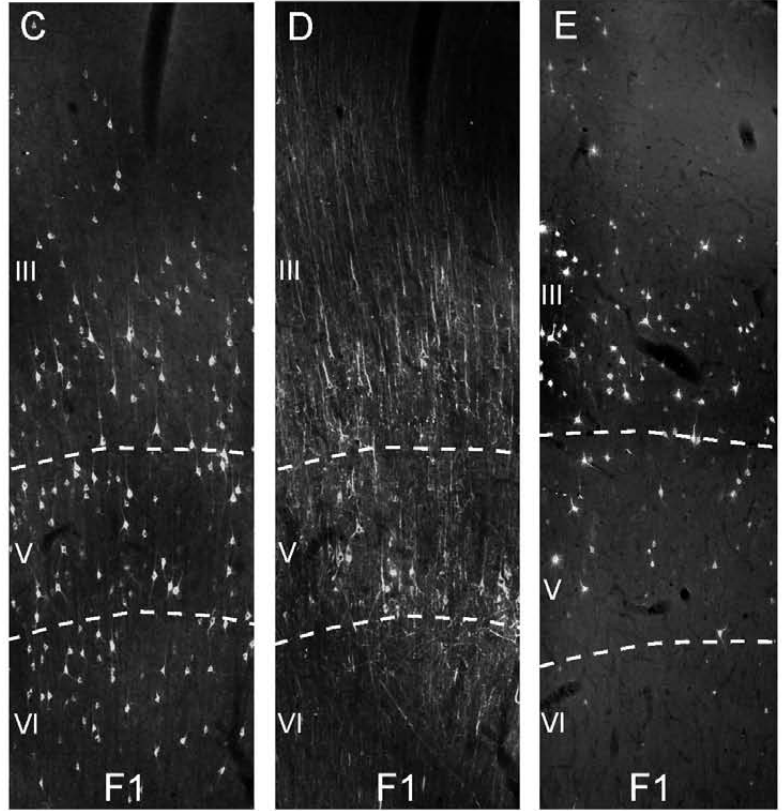




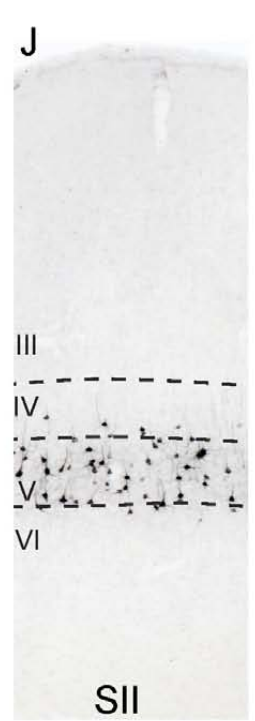
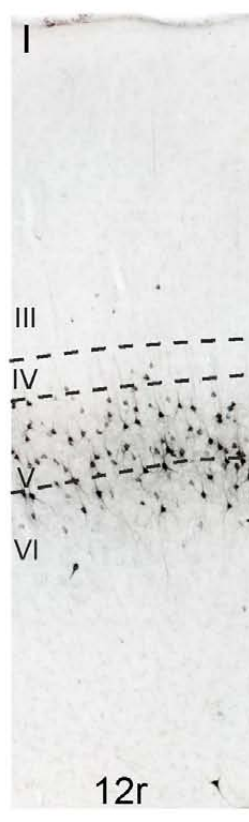




23 0.5 mm 23



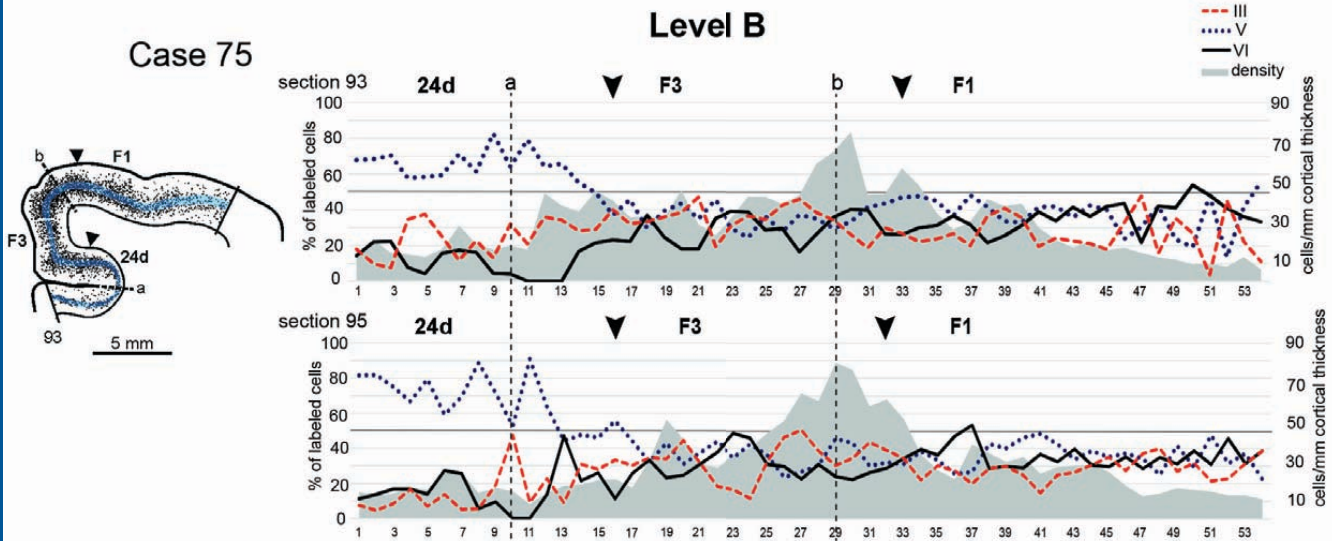
0.25 mm



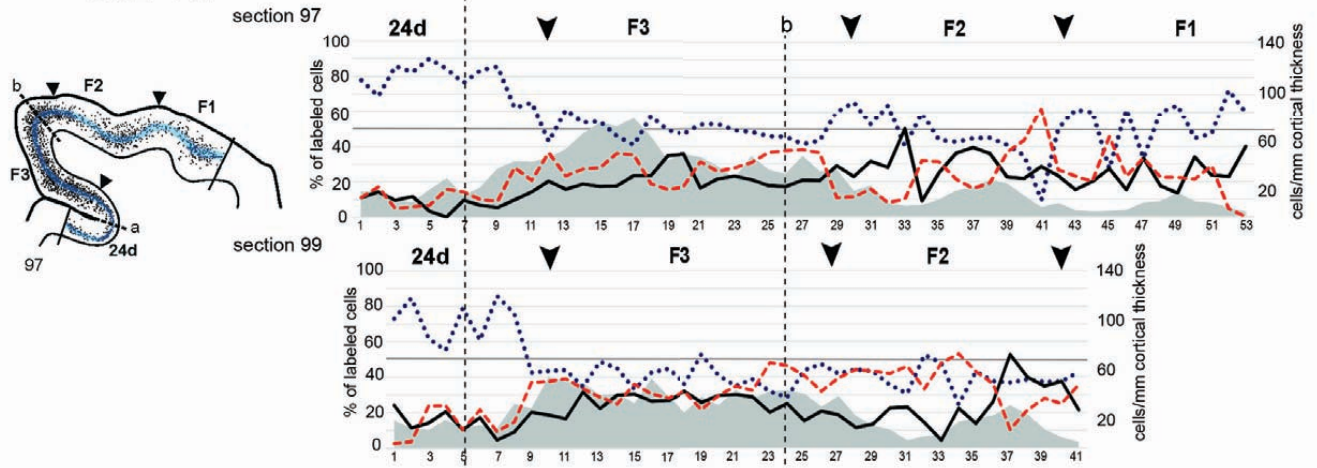


Case 75

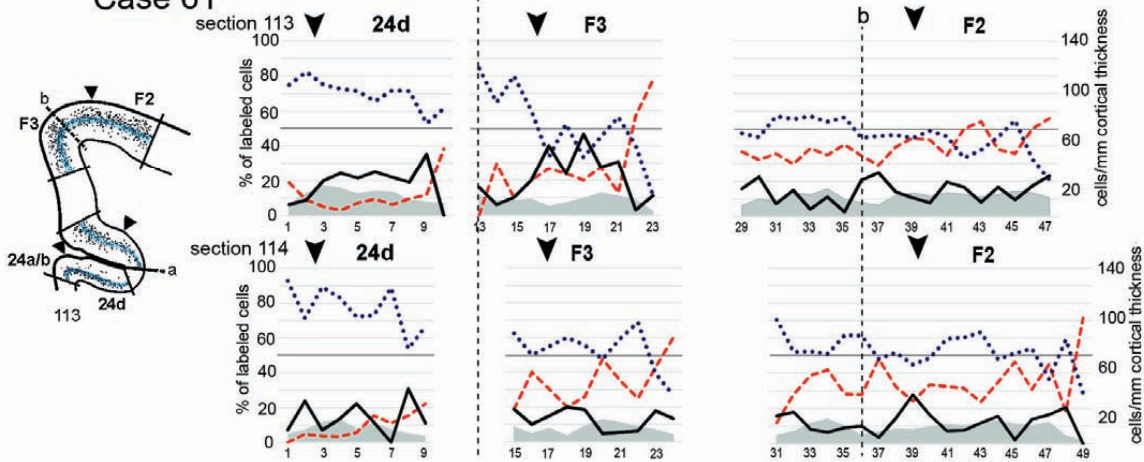
Level B

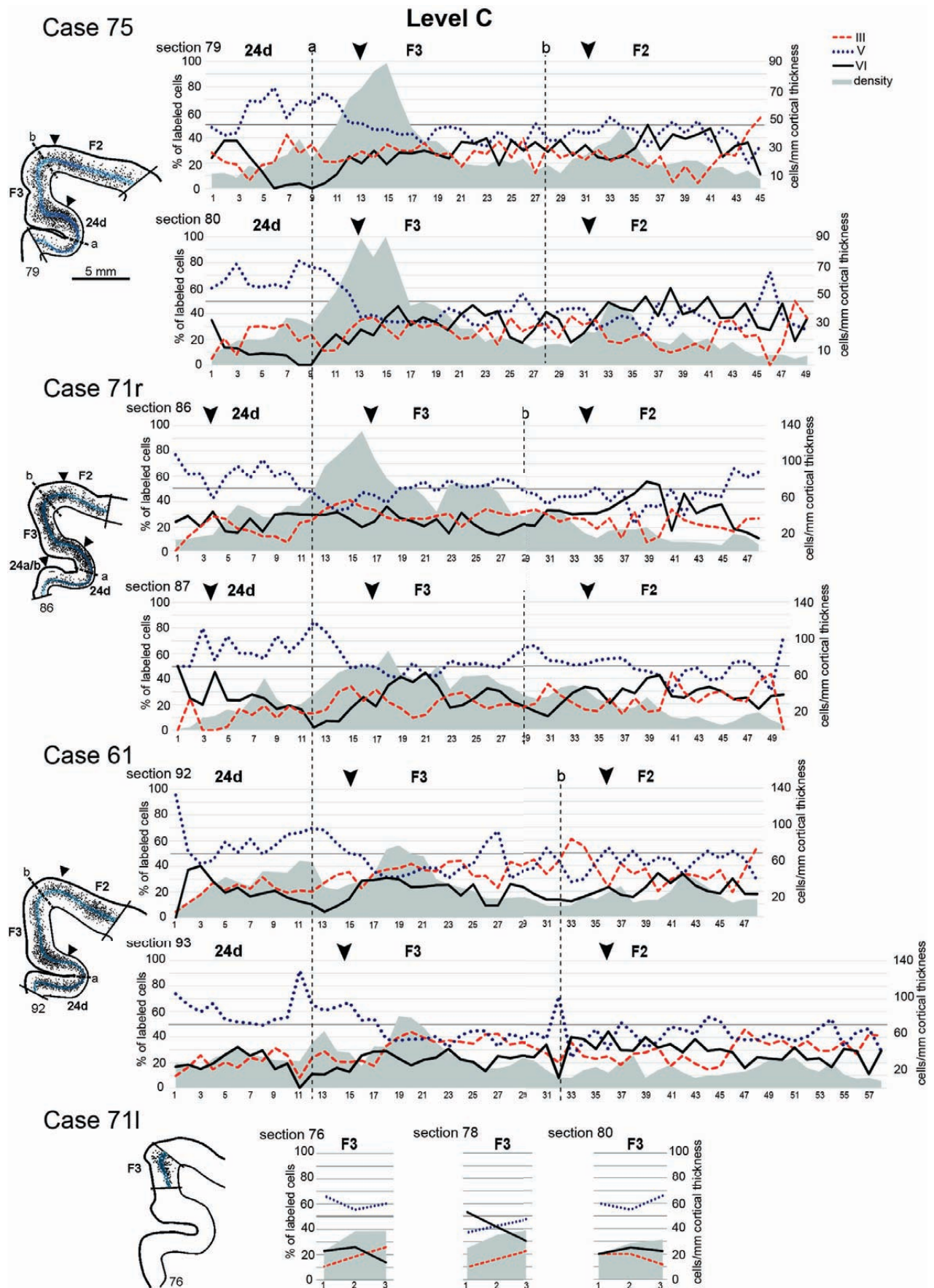


Case 71r



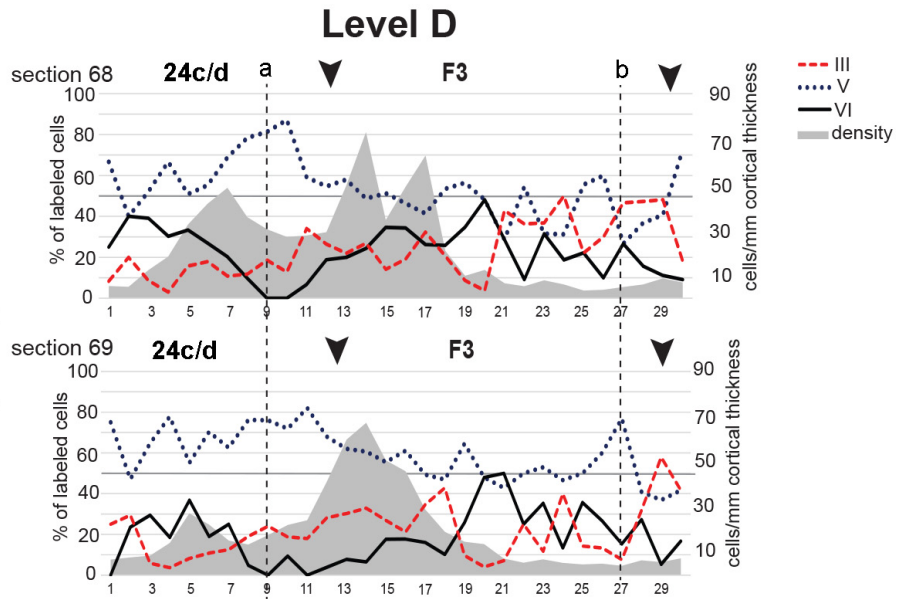
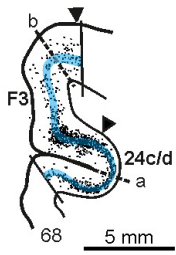
Case 61



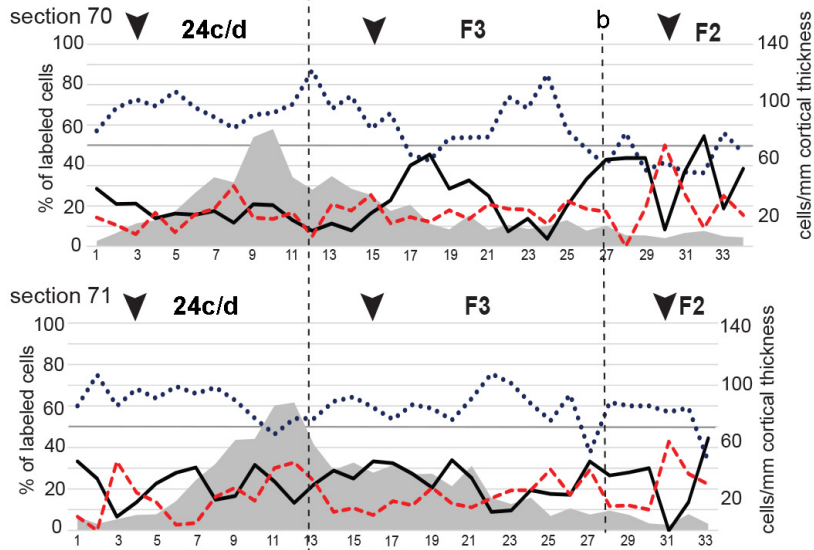
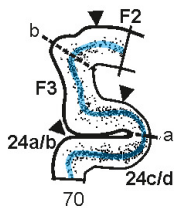




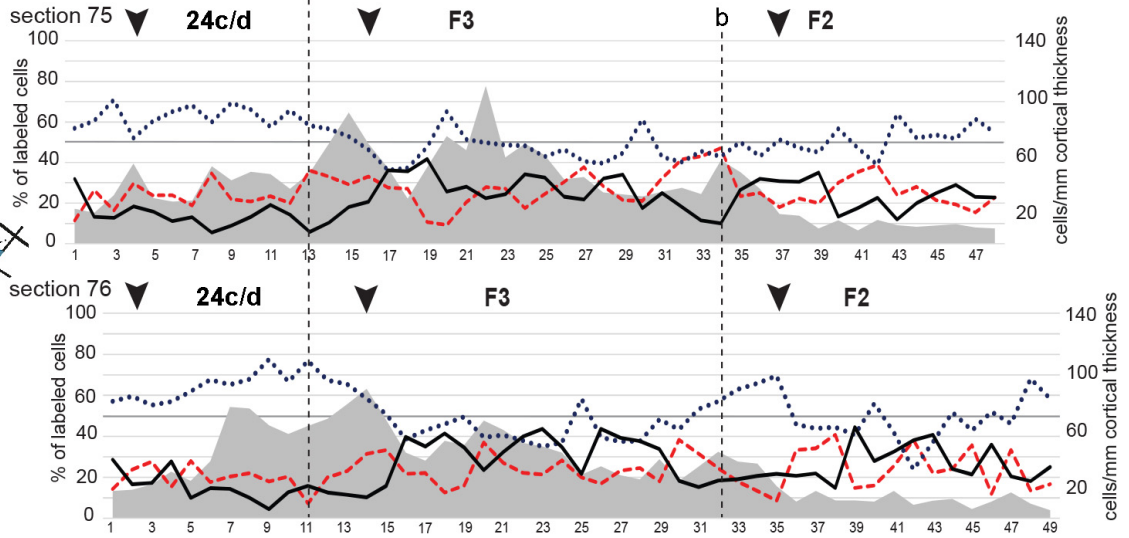
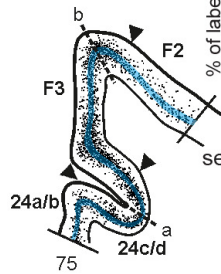
Case 75

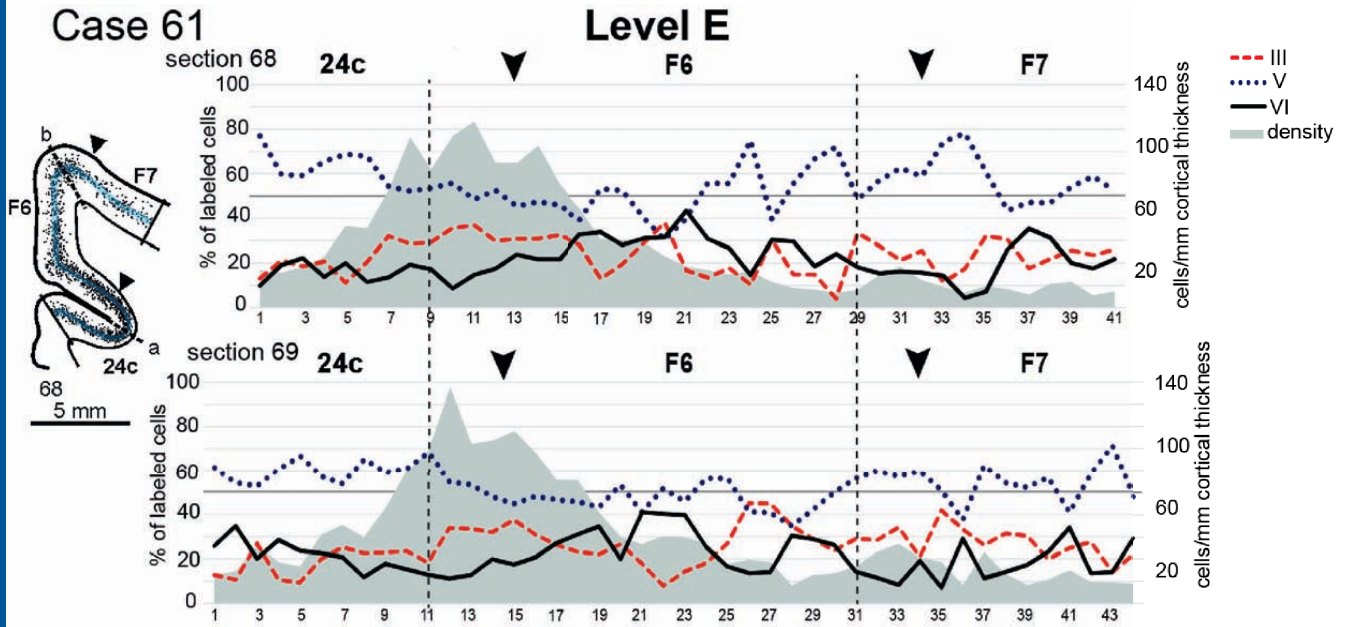


Case 71r



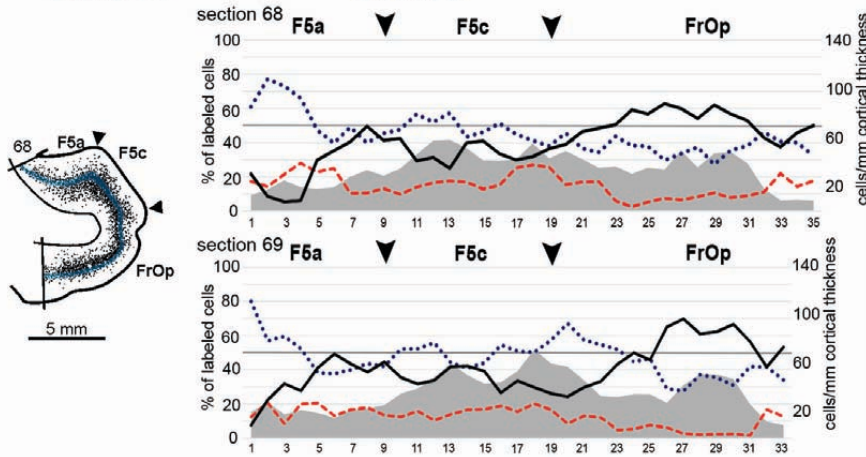
Case 61





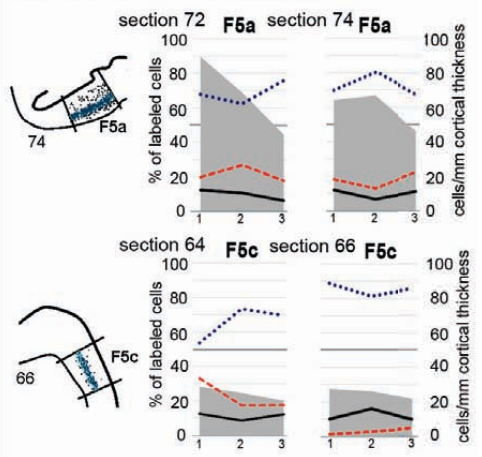
Case 61

Level E



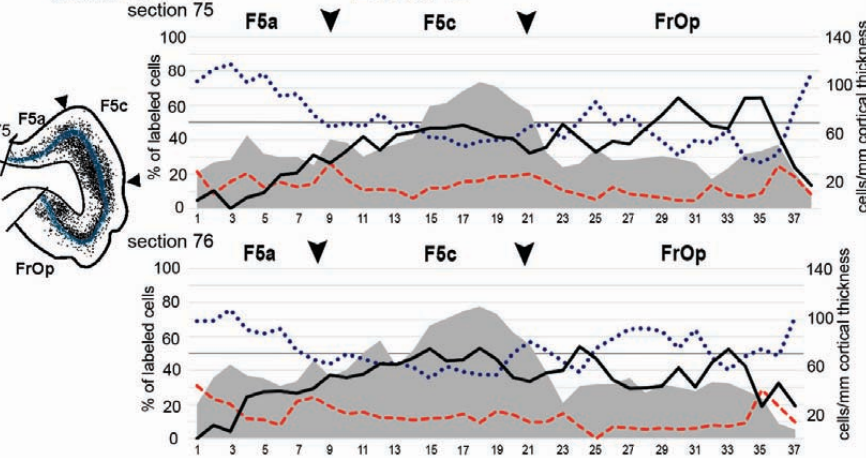
Case 71l

Level D



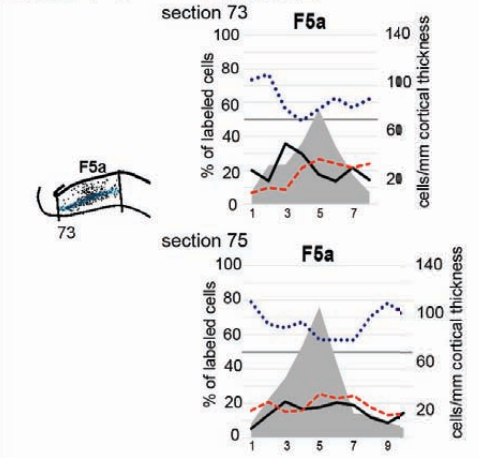
Case 61

Level D



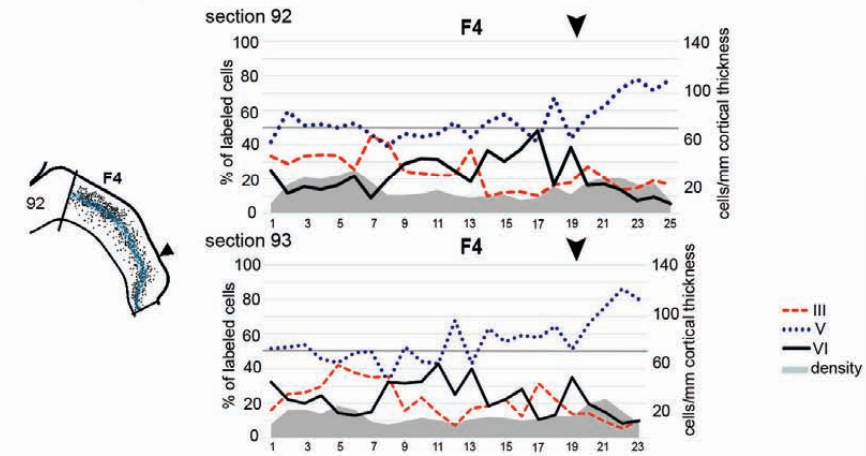
Case 71r

Level D



Case 61

Level C



Case 71r

Level C

